Living fossil or evolving virus?

Keizo Tomonaga

Although virus-like organisms are thought to have appeared together with the earliest forms of cellular life, their origin remains a mystery and we have little idea of the features of ancient viruses. Conversely, we know a lot about modern viruses, which show great diversity in genome organization and replication machinery, probably due to their antagonistic co-evolution with host defence mechanisms. However, not only is it extremely difficult to follow the details of these evolutionary processes, it is also hard to predict what ancient viruses might have been like, because only retroviruses have left a fossil record of their infection in hosts.

Against this background, the study of bornaviruses is shedding light on the murky past of viral origins and evolution. Bornaviruses are non-segmented, negative-strand RNA viruses that are characterized by their ability to infect nervous system cells without causing cell damage. A mammalian bornavirus, Borna disease virus (BDV), is infectious to a wide variety of host species and causes central nervous system disorders (Ikuta *et al*, 2002). Records dating to the seventeenth century in Germany, for example, detail neurological disorders in horses that we now know are caused by BDV infection.

The most striking feature of bornaviruses is that they establish a persistent infection in host cell nuclei, making them the only animal RNA virus capable of this type of intranuclear parasitism. Another important property of bornaviruses was uncovered recently by an international team of researchers (Horie *et al*, 2010): BDV was shown to integrate a DNA copy of its mRNA into the genetic material of the host in persistently infected cells. Although other non-retroviral RNA viruses are known to produce DNA versions of their genomes during replication (Klenerman *et al*, 1997; Geuking *et al*, 2009), bornaviruses are so far unique in having left endogenous fragments of themselves in the genomes of many mammalian species, including humans (Horie *et al*, 2010). At least four copies of these elements—homologous to the BDV nucleoprotein and thus named endogenous Borna-like nucleoprotein (EBLN)—have been found in the human genome, and their orthologues in the genomes of other primates. A phylogenetic analysis of these fragments has revealed that humans probably first acquired an EBLN fragment at least 40 million years ago. EBLN is therefore regarded as the first endogenous, non-retroviral viral element to be found in a mammalian genome, and it might preserve the features of ancestral bornaviruses.

Given this tantalizing possibility, the discovery of EBLN fragments has given rise to a host of new questions. The first surprise is the extremely long coexistence of bornaviruses and humans over 40 million years, in spite of which, we have not yet overcome their infection. More strangely, despite tens of millions of years spent replicating as exogenous viruses, the sequences of current bornaviruses are similar to those of EBLNs.

A main form of modern bornavirus infection is a chronic, life-long persistence in the host. Such a harmonious coexistence with the host might have enabled the virus to limit the accumulation of genetic variation during evolution. Of course, it is also possible that other events and processes—natural selection, recombination and switching to alternative host species—might also have been crucial in the conservation of bornavirus sequences. Is the modern bornavirus a living fossil that has retained the features of the ancient virus? Solving this puzzle of high sequence conservation is key to exploring the evolution and origin of RNA viruses.

The integration of BDV DNA into host genomes could represent a novel mode of pathogenesis in RNA virus infection. Persistent infection with BDV causes neurological disorders in animals in the absence of inflammation in the brain, which suggests that BDV directly induces the functional disturbance of infected neurons (Gonzalez-Dunia *et al*, 2005). Although the frequency of BDV integration into the host genome appears to be low, the functional disturbance caused by BDV might be a consequence of gene disruption due to the insertion of its DNA. This intriguing hypothesis is under investigation. Notably, some primate EBLNs are known to be expressed and to interact with several cellular proteins (Ewing *et al*, 2007); it will be interesting to determine their cellular function. It is also enticing to consider whether RNA viruses in general have had a role as drivers of genetic innovation or mutation during the evolution of their hosts.

The specific sequence characteristics of EBLNs and integrated BDV DNAs suggests that retrotransposons, such as the long interspersed nucleotide element 1 (L1) family, are involved in the integration of bornavirus sequences. This, in turn, suggests that EBLNs are processed pseudogenes derived from ancient bornaviruses. Yet, if L1s are responsible for bornavirus integration into the host genome, what ensures the specificity of L1s for bornavirus nucleoprotein mRNA without targeting other viral RNAs? This is one of many intriguing topics that remains to be explored; the unknown mechanism that enables bornavirus intranuclear residence could perhaps explain this specificity. The template switching of L1-encoded proteins was proposed recently as a mechanism of chimeric pseudogene formation from non-L1 cellular RNAs (Garcia-Perez *et al*, 2007). On the one hand, it is tempting to speculate that the bornavirus mRNA could be a target of this template-switching mechanism in the nucleus. On the other hand, a better control of bornavirus DNA integration into host genomes will also be necessary to make wide use of a recently established BDV-based vector system.

The study of such an ancient RNA virus will hopefully reinvigorate interest in this broad research area. A better understanding of the evolution of bornaviruses might provide clues as to the origin and/or evolution of RNA viruses in general.

REFERENCES

Ewing RM *et al* (2007) *Mol Syst Biol* **3:** 89
Garcia-Perez JL *et al* (2007) *Genome Res* **17:** 602–611
Geuking MB *et al* (2009) *Science* **323:** 393–396
Gonzalez-Dunia D *et al* (2005) *Virus Res* **111:** 224–234
Horie M *et al* (2010) *Nature* **436:** 84–87
Ikuta K *et al* (2002) *Front Biosci* **7:** D470–D495
Klenerman P, Hengartner H, Zinkernagel RM (1997) Nature **390:** 298–301

Keizo Tomonaga is at the Department of Virology at the Research Institute for Microbial Diseases, Osaka University, Osaka, Japan, and at PRESTO, Japan Science and Technology Agency, Tokyo, Japan.
E-mail: tomonaga@biken.osaka-u.ac.jp

EMBO *reports* (2010) **11,** 327. doi:10.1038/embor.2010.59

©2010 EUROPEAN MOLECULAR BIOLOGY ORGANIZATION

LETTERS

Endogenous non-retroviral RNA virus elements in mammalian genomes

Masayuki Horie[1]*, Tomoyuki Honda[1,2]*, Yoshiyuki Suzuki[3], Yuki Kobayashi[3], Takuji Daito[1], Tatsuo Oshida[4], Kazuyoshi Ikuta[1], Patric Jern[5], Takashi Gojobori[3], John M. Coffin[5] & Keizo Tomonaga[1,6]

Retroviruses are the only group of viruses known to have left a fossil record, in the form of endogenous proviruses, and approximately 8% of the human genome is made up of these elements[1,2]. Although many other viruses, including non-retroviral RNA viruses, are known to generate DNA forms of their own genomes during replication[3–5], none has been found as DNA in the germline of animals. Bornaviruses, a genus of non-segmented, negative-sense RNA virus, are unique among RNA viruses in that they establish persistent infection in the cell nucleus[6–8]. Here we show that elements homologous to the nucleoprotein (N) gene of bornavirus exist in the genomes of several mammalian species, including humans, non-human primates, rodents and elephants. These sequences have been designated endogenous Borna-like N (EBLN) elements. Some of the primate EBLNs contain an intact open reading frame (ORF) and are expressed as mRNA. Phylogenetic analyses showed that EBLNs seem to have been generated by different insertional events in each specific animal family. Furthermore, the EBLN of a ground squirrel was formed by a recent integration event, whereas those in primates must have been formed more than 40 million years ago. We also show that the *N* mRNA of a current mammalian bornavirus, Borna disease virus (BDV), can form EBLN-like elements in the genomes of persistently infected cultured cells. Our results provide the first evidence for endogenization of non-retroviral virus-derived elements in mammalian genomes and give novel insights not only into generation of endogenous elements, but also into a role of bornavirus as a source of genetic novelty in its host.

Bornaviruses are the only animal RNA viruses that achieve a highly cell-associated life cycle within the nuclear envelope[6–9], and can therefore provide not only new models of RNA virus replication, but also insight into dynamics of RNA molecules in eukaryote cells. In an effort to understand whether bornaviruses mimic host factors to maintain persistent infection in the nucleus, we searched human protein databases for sequences with similarity to BDV proteins. This search identified two hypothetical human proteins (GeneID LOC340900 and LOC55096), each of which has significant sequence similarity to BDV N (Fig. 1a and Supplementary Table 1). BDV N is a major structural protein, which tightly encapsidates the viral RNA to form the nucleocapsid. The LOC340900 sequence encodes a protein of comparable length (366 residues) to BDV N (370 residues), whereas LOC55096 seems to contain several frameshift mutations relative to BDV N, resulting in a shorter ORF length (Fig. 1a). Both LOC340900 and LOC55096 showed an overall 41% sequence identity and 58% similarity to BDV N and 72% identity to each other. The close relationship between BDV N and the homologous genes was further demonstrated by the alignment of transcription regulatory sequences on either side of BDV N (Fig. 1b). The S and T motifs in flanking sequences of both putative human proteins were well conserved with those of BDV (Fig. 1b). In addition, a poly-A sequence appears after the T1-like motif in the 3′ flanking region of LOC55096 (Fig. 1b). The homology of the human genes to BDV N was also confirmed by a permutation test (Supplementary Fig. 1). These findings indicated that both human genes may be endogenous elements related to BDV N gene, and therefore we designated them EBLNs (LOC340900, EBLN-1 and LOC55096, EBLN-2).

To investigate the presence of EBLN sequences in other animal species, we conducted tblastn searches using BDV N as a query in eukaryote and whole-genome shotgun databases at NCBI. Sequences with blast *E*-values of 10^{-10} or lower were identified as EBLNs. We found two additional human elements (EBLN-3 and -4) as well as a number of related sequences in various mammalian species, including marsupials (Supplementary Table 2). Orthologous genes to human EBLNs were identified in the genomes of non-human anthropoid primates, including chimpanzee, gorilla, orang-utan, and macaque (Supplementary Table 2). We also detected primate EBLNs in the genomes of the suborder Strepsirrhini, including the mouse lemur and Garnett's galago. Furthermore, two species of the Afrotheria, African elephant and cape hyrax, and four rodents were found to have EBLNs with *E*-values of less than 10^{-20} (Supplementary Table 2). An EBLN locus with a high level of similarity to BDV N was also identified in the thirteen-lined ground squirrel (TLS) genome (Supplementary Fig. 2a). Like the human EBLNs, the TLS EBLN contained a 3′ poly-A sequence, as well as S and T signal motifs, in its 3′ flanking region (Supplementary Fig. 2b). Almost all EBLN fragments, except for EBLN-1 and the TLS gene, contained several stop codons in the predicted coding sequences, or lacked the identifiable flanking sequences. In addition, we found that all anthropoid EBLNs, except for EBLN-4, are expressed as mRNAs in some human and monkey-derived cell lines (Supplementary Fig. 3). A previous study reported the interaction of human EBLN-2 with other cellular proteins, such as AP1S1, TUSC2/FUS1 and FANCC (ref. 10) (Supplementary Table 1), indicating that anthropoid EBLNs may encode functional proteins.

To investigate whether other mammalian species contain EBLN-related sequences in their genomes further, we conducted Southern blot hybridization under low-stringency conditions using human, murine and TLS EBLN as probes (Fig. 1c and d). Along with the clear signals in primate genomes, we detected reproducible faint positive bands in murine and shrew genomes when using a human EBLN probe (Fig. 1c, dots). The signals were also observed using a mouse

[1]Department of Virology, Research Institute for Microbial Diseases (BIKEN), Osaka University, Osaka 565-0871, Japan. [2]Japan Society for the Promotion of Science (JSPS), Chiyoda-ku, Tokyo 102-8472, Japan. [3]Center for Information Biology and DNA Data Bank of Japan, National Institute of Genetics, Mishima, Shizuoka 411-8540, Japan. [4]Department of Life Science and Agriculture, Obihiro University of Agriculture and Veterinary Medicine, Obihiro, Hokkaido 080-8555, Japan. [5]Department of Molecular Biology and Microbiology, Tufts University School of Medicine, Boston, Massachusetts 02111, USA. [6]PRESTO, Japan Science and Technology Agency (JST), Chiyoda-ku, Tokyo 102-0075, Japan.
*These authors contributed equally to this work.

©2010 Macmillan Publishers Limited. All rights reserved

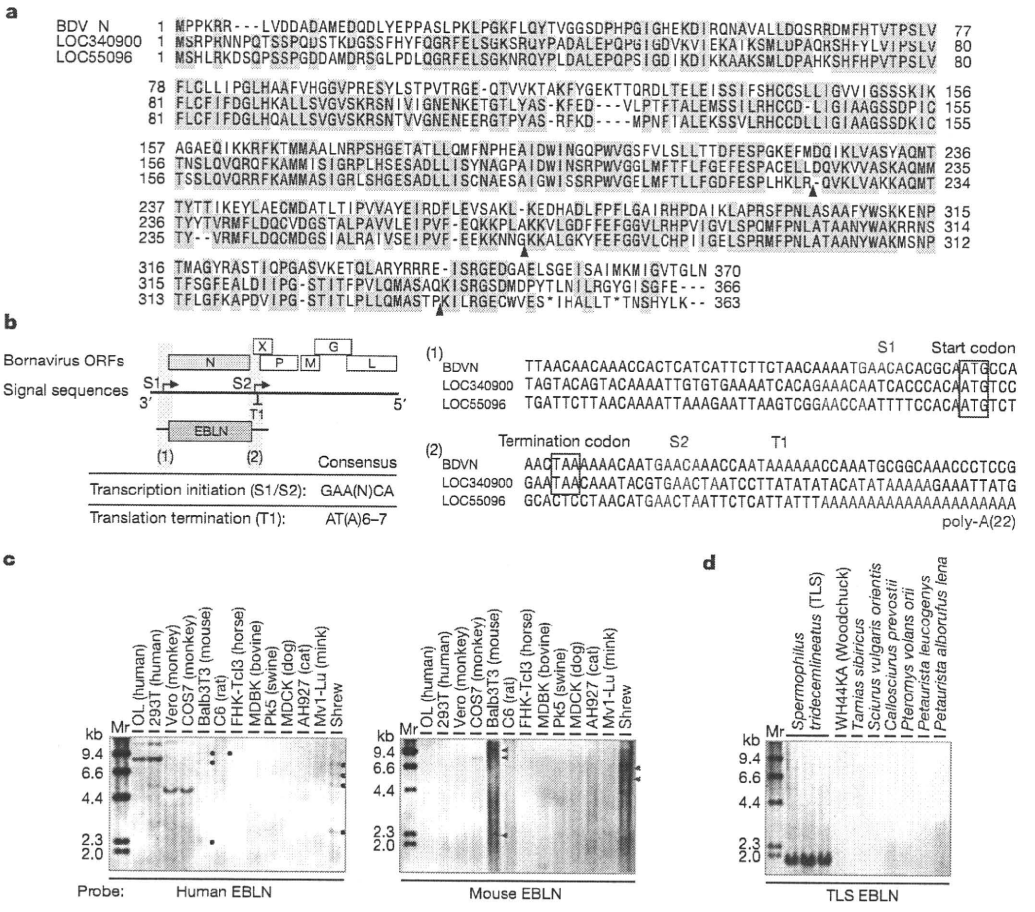

Figure 1 | Bornavirus N-like elements in mammalian genomes. **a**, Alignment between predicted amino acid sequences of BDV N and two human bornavirus N-like elements. Black arrowheads indicate predicted frameshift sites in LOC55096. **b**, Sequence alignments of transcription signal sites (S1/S2 and T1) at both the 5′ and 3′ ends of the bornavirus N ORF. A schematic representation of bornavirus genome structure is shown. **c**, **d**, Low-stringency Southern blot hybridizations of DNA from various mammalian species using human EBLN-1 and mouse EBLN chr.11 (**c**) and TLS EBLN (**d**) as probes. Dots and arrowheads on the right side of the murine and shrew lanes in panel **c** indicate the positions of reproducible positive signals. Mr, Molecular marker.

EBLN probe (Fig. 1c, arrowheads), indicating that the faint bands are most likely to be EBLN-related sequences. In fact, EBLN-like sequences, albeit with *E*-values greater than 10^{-10}, were found in the Eurasian shrew genome in our tblastn searches. On the other hand, except for TLS, no positive band was detected by the TLS probe in the genomes of several different squirrel species, such as woodchuck (*Marmota* spp.), the closest species to the TLS (*Spermophilus* spp.) (Fig. 1d)[11], indicating that the ground squirrels are likely to be the only host species of EBLN within the squirrel family. The BDV N probe detected many faint and smear bands that include the signals detected by EBLN-specific probes in both selected mammalian species and the squirrel families (Supplementary Fig. 4), indicating that EBLN-related fragments are more widely distributed in the mammalian genome.

We next performed a comprehensive phylogenetic analysis using nucleotide sequences of all EBLNs with *E*-values less than 10^{-20} (Fig. 2 and Supplementary Fig. 5). In addition to EBLNs, we included avian bornaviruses (ABVs)[12] and an exogenous reptile bornavirus (RBV) sequence, which was detected in a cDNA library from a *Bitis gabonica* (Gaboon viper) venom gland[13] (Supplementary Fig. 6). As shown in Fig. 2, the anthropoid and murine EBLNs are clustered phylogenetically within each host order. By contrast, EBLNs from other species, including African elephant, cape hyrax and guinea pig, form branches independent from the evolutionary lineage of their hosts, indicating that these EBLNs had most likely invaded each species via independent integration events. Interestingly, the TLS EBLNs form a tight cluster more closely related to modern exogenous bornaviruses than to those of other animals. Considering that a closely related species does not contain EBLNs, the integration of squirrel EBLN could have been a very recent event. A phylogenetic analysis using all primate EBLNs, including marmoset (Supplementary Fig. 7), showed that the integration events leading to the primate EBLNs occurred in the Haplorrhini at least before the split between rhesus macaque and marmoset.

To investigate whether current bornaviruses are able to be copied into DNA to produce EBLN-like elements, we first performed PCR analyses using DNA of persistently BDV-infected cells. As shown in Fig. 3a and Supplementary Table 3, BDV DNA was clearly detected in some cell lines by a primer set targeted to the BDV N region. To understand which viral RNA species serve as template for the DNA form of BDV, we used several primers within the BDV genome for amplification. The results showed that primer sets straddling the boundaries of BDV transcription units could not amplify BDV-specific DNA (Fig. 3b and c), indicating that the DNA is transcribed from mRNAs of BDV. We detected BDV-specific DNA in the brains of persistently BDV-infected mice (Supplementary Fig. 8), indicating that BDV can produce DNA forms *in vitro* and *in vivo*. We next performed Alu-PCR to investigate whether BDV DNA detected in the infected cells exists as integrated or extrachromosomal DNA. As shown in Fig. 3d and Supplementary Fig. 9, an Alu-specific PCR product was detected in BDV-infected cells only when using an N-specific forward primer about 30 days post-infection. This observation indicated that although BDV DNA in infected cells may be mainly extrachromosomal, the N gene is integrated into the host genome during persistent infection.

We further characterized the BDV DNA insertions and flanking cellular sequences by using Alu-PCR and inverse PCR (Supplementary Fig. 10)[14]. Integration sites were present on various chromosomes

©2010 Macmillan Publishers Limited. All rights reserved

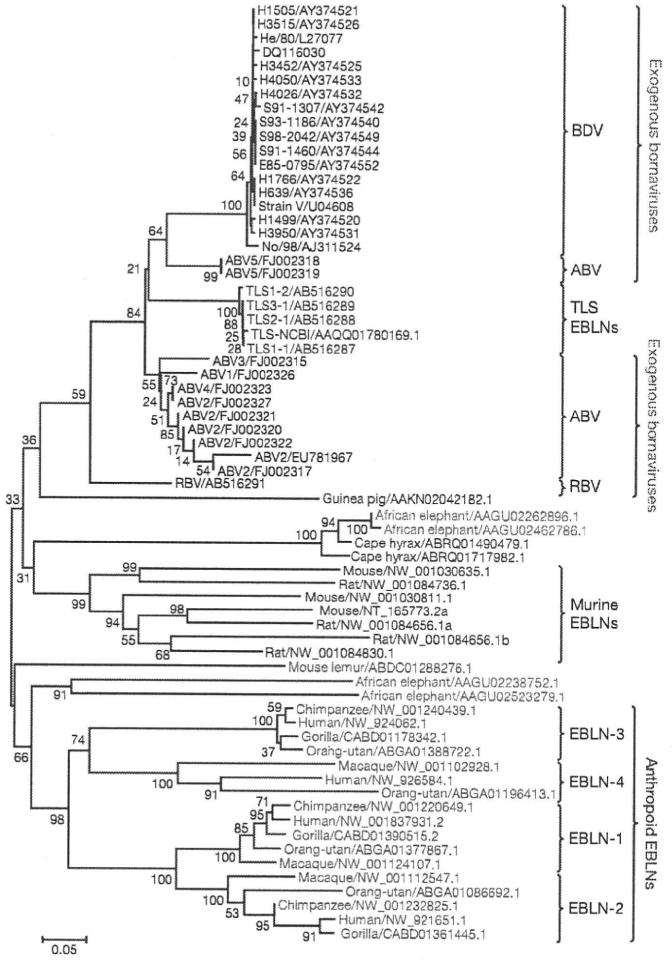

Figure 2 | Phylogenetic tree of exogenous bornaviruses and mammalian EBLNs. The bootstrap probability is indicated for each interior branch. The scale bar indicates the number of amino acid substitutions per site. Animals belonging to the same order are indicated by the same colour. Strain and sequence accession numbers are given for each sequence.

(Fig. 4). Similar to some mammalian EBLNs, many BDV DNA insertions contained a 3′ poly-A sequence (Fig. 4b and c). In addition, integrations of truncated BDV N DNA were also found in some clones. No apparent consensus sequences were found at the sites, although target site duplications (TSDs) were detected in some clones from the inverse PCR (Fig. 4c). We also found deletions, as well as sequence rearrangement, of host genome adjacent to BDV DNA insertions (Fig. 4c). These results indicate that modern BDV is able to produce DNA forms leading to insertion of EBLN-like elements into its host's genome.

This report is the first to provide evidence of endogenous sequences derived from a non-retroviral RNA virus in mammalian species. Phylogenetic analyses demonstrate that the oldest primate EBLN observed must have appeared in an ancestor of primates after the separation between Strepsirrhini and Haplorrhini, implying that bornaviruses have coexisted with primates for an evolutionary history stretching at least 40 million years. Thus, bornaviruses are the first non-retroviral RNA virus whose existence in prehistoric times has been confirmed. To date, the evolution/origin of RNA viruses is a major puzzle in the relationship between viruses and mammalian hosts, because simple molecular clock calculations using an average rate of nucleotide substitutions estimate the origin of RNA viruses to be a very recent event[15–17]. Despite replication during tens of millions of years as exogenous viruses, the amino acid sequences of current BDV N seem surprisingly conserved relative to EBLNs. This conservation demonstrates the inapplicability of simple molecular clocks to RNA virus evolution. Discovery of EBLNs in several

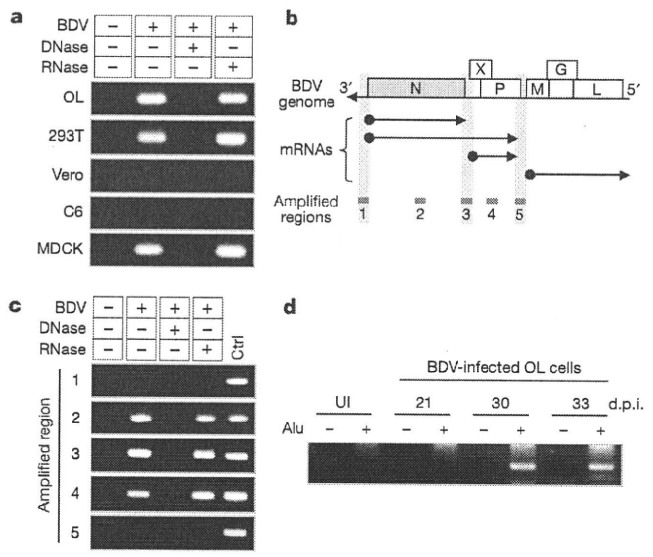

Figure 3 | Reverse transcription and integration of BDV RNA in mammalian cells. **a**, PCR amplification of BDV N-specific cDNA in BDV-infected cells. OL and 293T, human; Vero, monkey; C6, rat; MDCK, dog. **b**, Schematic representation of the bornavirus genome and mRNAs. Regions for the PCR amplification are indicated by red bars. **c**, Region-dependent amplification of BDV cDNA in infected OL cells. The numbers on the left side of the panels correspond to the amplification regions in panel **b**. Ctrl indicates the results of RT–PCR using RNA from BDV-infected OL cells. **d**, Integration of BDV DNA. Genomic DNA was isolated from BDV-infected OL cells at the indicated days after infection, and Alu-PCR was performed with (+) or without (–) the Alu primer. UI, genomic DNA from uninfected cells; d.p.i., days post-infection.

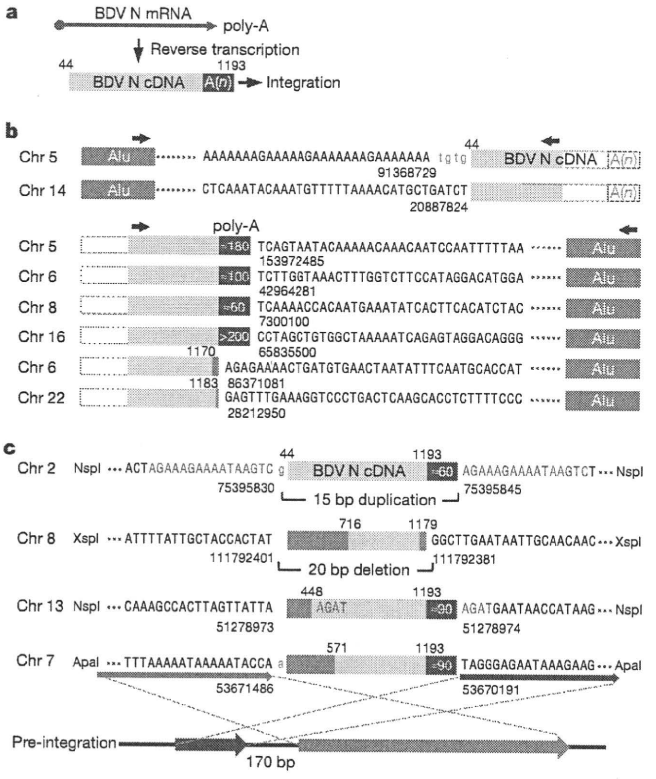

Figure 4 | Structures of BDV N integration events in OL cells. **a**, Structure of BDV N cDNA. The numbering corresponds to nucleotide positions in the BDV genome. The BDV N transcript runs from nucleotide positions 44 to 1193. **b, c**, Structures of BDV N integrations detected by Alu-PCR (**b**) and inverse PCR (**c**). Grey rectangles in the N cDNA indicate truncated regions. Black lettering, host genome sequences; green lettering, inserted nucleotides; red lettering, predicted TSDs. The blue box indicates the position and length of the poly-A sequence. The pre-integration form of chromosome 7 is shown in panel **c**.

©2010 Macmillan Publishers Limited. All rights reserved

mammalian species will help shed light on the evolutional history of RNA viruses and their hosts.

The sequence characteristics of both EBLNs and BDV DNA insertions in host genomes indicate that the reverse transcriptase activity encoded by retrotransposons, such as long interspersed nucleotide elements (LINEs), is likely to be involved in the reverse transcription and integration of bornavirus mRNAs, although some clones showed no apparent TSDs (ref. 18). LINE-1s (L1) are abundant retrotransposons, whose enzymes are able to sometimes target cellular mRNAs and produce processed pseudogenes in mammalian genomes[19–21]. The organization of sequences flanking EBLN-2 is consistent with the action of L1. The sequence shows the presence of an AluSx element immediately downstream of the 3′ poly-A tail of EBLN-2 (Supplementary Fig. 11). The key observation is that the EBLN-2/AluSx element is flanked by a perfect 9-bp TSD. Because the AluSx itself is not flanked by TSDs and the 3′ end of Alu is known to be recognized by L1 during target-primed reverse transcription, the presumed EBLN-2/AluSx chimaera element was most likely created and integrated by the L1 machinery. Thus, it is likely that EBLNs are processed pseudogenes derived from ancient bornavirus infections. At present, the reasons why bornaviruses but not other non-retroviral RNA viruses, and why only N and not other genes, have been preserved in mammalian genomes as endogenous elements are not clear. There are several possibilities. First, bornaviruses may have greater access to the germline. Second, the BDV N mRNA, like some cellular RNAs, may have features that, by chance, make it a favourable template for L1-mediated reverse transcription[22,23]. Third, the predominant transcription of BDV N mRNA in infected cells may also favour its association with the L1 replication machinery. The selectivity for BDV N mRNA implies a role for specific structural features, perhaps in conjunction with one or more of the other possibilities. Our data also raise the possibility that, like some endogenous retroviruses, EBLNs may have some function in their host species. An analysis of the non-synonymous to synonymous substitution ratios among anthropoid EBLNs indicates functional, albeit weak, evolutionary conservation. This finding implicates bornaviruses as a new source of genetic innovation in their hosts. Further studies will be needed to explore this possibility.

METHODS SUMMARY

Homology searches (blastp, tblastn) were conducted using the amino acid sequence of BDV N H1499 (International Nucleotide Sequence Database accession number AY374520) as a query and the genomic sequences of 234 eukaryotes as a database at the genomic blast server at the National Center for Biotechnology and Information, NCBI. Sequence hits with *E*-values less than 10^{-10} were collected together with neighbouring hits, if any, with higher *E*-values and combined according to their alignment pattern with BDV N. The resulting amino acid sequence was examined for the presence of a BDV_P40 domain (Pfam accession number PF06407.3) using HMMPFAM. The sequence was identified as a putative EBLN when the domain was detected with the *E*-value of less than 10^{-10}.

The putative EBLN amino acid sequences that were identified with *E*-value of less than 10^{-20} in both tblastn and HMMPFAM were used for the phylogenetic analysis with N sequences of various exogenous bornaviruses. The multiple alignments of EBLN and BDV N amino acid sequences were made according to the alignment pattern of EBLN sequences to BDV N in the tblastn results. The phylogenetic tree was constructed using the neighbour-joining method[24] and the evolutionary distance measured as the proportion of difference (*p* distance) with the pairwise deletion option in MEGA (version 4.0)[25]. The reliability of interior branches in the phylogenetic tree was assessed by the bootstrap method with 1,000 resamplings.

Full Methods and any associated references are available in the online version of the paper at www.nature.com/nature.

Received 2 September; accepted 17 November 2009.

1. Jern, P. & Coffin, J. M. Effects of retroviruses on host genome function. *Annu. Rev. Genet.* **42**, 709–732 (2008).
2. International Human Genome Sequencing Consortium. Initial sequencing and analysis of the human genome. *Nature* **409**, 860–921 (2001).
3. Zhdanov, V. M. Integration of viral genomes. *Nature* **256**, 471–473 (1975).
4. Klenerman, P., Hengartner, H. & Zinkernagel, R. M. A non-retroviral RNA virus persists in DNA form. *Nature* **390**, 298–301 (1997).
5. Geuking, M. B. *et al.* Recombination of retrotransposon and exogenous RNA virus results in nonretroviral cDNA integration. *Science* **323**, 393–396 (2009).
6. Tomonaga, K., Kobayashi, T. & Ikuta, K. Molecular and cellular biology of Borna disease virus infection. *Microbes Infect.* **4**, 491–500 (2002).
7. de la Torre, J. C. Molecular biology of Borna disease virus and persistence. *Front. Biosci.* **7**, d569–d579 (2002).
8. Lipkin, W. I. & Briese, T. in *Fields Virology* 5th edn (eds Knipe, D. M. & Howley, P. M.) 1829–1851 (Lippincott Williams & Wilkins, 2007).
9. Chase, G. *et al.* Borna disease virus matrix protein is an integral component of the viral ribonucleoprotein complex that does not interfere with polymerase activity. *J. Virol.* **81**, 743–749 (2007).
10. Ewing, R. M. *et al.* Large-scale mapping of human protein–protein interactions by mass spectrometry. *Mol. Syst. Biol.* **3**, 89 (2007).
11. Mercer, J. M. & Roth, V. L. The effects of Cenozoic global change on squirrel phylogeny. *Science* **299**, 1568–1572 (2003).
12. Kistler, A. L. *et al.* Recovery of divergent avian bornaviruses from cases of proventricular dilatation disease: identification of a candidate etiologic agent. *Virol. J.* **5**, 88 (2008).
13. Francischetti, I. M., My-Pham, V., Harrison, J., Garfield, M. K. & Ribeiro, J. M. Bitis gabonica (Gaboon viper) snake venom gland: toward a catalog for the full-length transcripts (cDNA) and proteins. *Gene* **337**, 55–69 (2004).
14. Hui, E. K., Wang, P. C. & Lo, S. J. Strategies for cloning unknown cellular flanking DNA sequences from foreign integrants. *Cell. Mol. Life Sci.* **54**, 1403–1411 (1998).
15. Holmes, E. C. Molecular clocks and the puzzle of RNA virus origins. *J. Virol.* **77**, 3893–3897 (2003).
16. Duffy, S., Shackelton, L. A. & Holmes, E. C. Rates of evolutionary change in viruses: patterns and determinants. *Nature Rev. Genet.* **9**, 267–276 (2008).
17. Korber, B., Theiler, J. & Wolinsky, S. Limitations of a molecular clock applied to considerations of the origin of HIV-1. *Science* **280**, 1868–1871 (1998).
18. Morrish, T. A. *et al.* DNA repair mediated by endonuclease-independent LINE-1 retrotransposition. *Nature Genet.* **31**, 159–165 (2002).
19. Maestre, J., Tchenio, T., Dhellin, O. & Heidmann, T. mRNA retroposition in human cells: processed pseudogene formation. *EMBO J.* **14**, 6333–6338 (1995).
20. Esnault, C., Maestre, J. & Heidmann, T. Human LINE retrotransposons generate processed pseudogenes. *Nature Genet.* **24**, 363–367 (2000).
21. Kazazian, H. H. Jr. Mobile elements: drivers of genome evolution. *Science* **303**, 1626–1632 (2004).
22. Zhang, Z., Carriero, N. & Gerstein, M. Comparative analysis of processed pseudogenes in the mouse and human genomes. *Trends Genet.* **20**, 62–67 (2004).
23. Pavlicek, A. & Jurka, J. in *Genomic disorders* (eds Lupski, J. R. & Stankiewicz, P.) 57–72 (Humana Press, 2006).
24. Saitou, N. & Nei, M. The neighbor-joining method: a new method for reconstructing phylogenetic trees. *Mol. Biol. Evol.* **4**, 406–425 (1987).
25. Tamura, K., Dudley, J., Nei, M. & Kumar, S. MEGA4: molecular evolutionary genetics analysis (MEGA) software version 4.0. *Mol. Biol. Evol.* **24**, 1596–1599 (2007).

Supplementary Information is linked to the online version of the paper at www.nature.com/nature.

Acknowledgements We thank A. Kawahara for helping the capture of the wild shrews (*Sorex unguiculatus* and *Sorex gracillimus*) at Kiritappu wetland, Hokkaido, Japan. We thank I. Francischetti for provision of Gaboon viper (*Bitis gabonica*) venom gland tissue and a cDNA library, D. Vaughan for thirteen-lined ground squirrel (*Spermophilus tridecemlineatus*) brain and liver tissues, and K. Maeda, T. Miyazawa and N. Ohtaki for providing culture cell lines from several mammalian species. This work was supported by the Ministry of Education, Culture, Sports, Science and Technology (MEXT) Grants-in-aid for Scientific Research on Priority Areas (Infection and Host Responses; Matrix of Infection Phenomena) (K.T.), PRESTO (RNA and Biofunctions) from Japan Science and Technology Agency (JST) (K.T.), a Health Labour Sciences Research Grants for Research on Measures for Intractable Diseases (H20 nanchi ippan 035) from the Ministry of Health, Labor and Welfare of Japan (K.T.), research grant R37 CA 089441 from the National Cancer Institute (J.M.C.) and a fellowship from the Wenner-Gren Foundation (P.J.). J.M.C. was a Research Professor of the American Cancer Society with support from the George Kirby Foundation.

Author Contributions K.T. designed research; M.H., T.H., T.D. and K.T. conducted experiments using virus and culture systems; T.O. collected samples; Y.S., Y.K. and T.G. performed phylogenetic analysis; M.H., T.H., Y.S., K.I., P.J., T.G., J.M.C. and K.T. analysed data; and M.H., Y.S., P.J., J.M.C. and K.T. wrote the manuscript. All authors discussed the results.

Author Information The TLS EBLN and RBV sequences reported here have been deposited in the DDBJ/EMBL/GenBank and the accession numbers are shown in Figure 2. Reprints and permissions information is available at www.nature.com/reprints. The authors declare no competing financial interests. Correspondence and requests for materials should be addressed to K.T. (tomonaga@biken.osaka-u.ac.jp).

©2010 Macmillan Publishers Limited. All rights reserved

METHODS

Permutation test. A permutation test was conducted to examine the homology of human EBLNs to the N gene of BDV, taking into account their base composition. The nucleotide sequence of each EBLN was aligned with that of the BDV N gene (strain CRP3A: accession number AY114161) using CLUSTAL W. Gaps were eliminated from the alignment, and the proportion of identical sites (q) was computed. Nucleotide sequences of both the EBLN and the BDV N gene were randomly permuted using pseudorandom numbers, and the q value was computed as indicated above. The permutation process was repeated 10,000 times, and the distribution of the q value between two unrelated sequences of the same base composition as the original EBLN and the N gene was obtained. The probability (p) of observing the q value equal to or greater than the original value in the comparison of unrelated sequences was obtained from the distribution.

Tissue samples. Tissues from three weanling thirteen-lined ground squirrel (*Spermophilus tridecemlineatus*) born in May 2008 (four generations from wild stock) were provided from the Ground Squirrel Captive Breeding Colony at the University of Wisconsin Oshkosh, USA. Immediately after decapitation, brain and liver were rapidly dissected, cut into 5 mm cubes, immersed in chilled methanol, and stored frozen in liquid nitrogen until use. Shrew tissues (brain and liver) were isolated from wild-captured long-clawed shrews (*Sorex unguiculatus*) in Hokkaido, Japan. The shrews were captured under sampling permission of the government of Hokkaido. Immediately after capture, tissue samples were fixed in RNAlater (Ambion) and stored frozen until use. Gaboon viper (*Bitis gabonica*) venom gland tissue was obtained as frozen samples from the Laboratory of Malaria and Vector Research at National Institute of Allergy and Infectious Diseases, National Institutes of Health, USA. Ethanol-fixed tissues from Siberian flying squirrels (*Pteromys volans orii*) and Eurasian red squirrels (*Sciurus vulgaris orientis*) were obtained from the Department of Life Science and Agriculture, Obihiro University of Agriculture and Veterinary Medicine, Obihiro, Hokkaido, Japan.

DNA isolation. Total DNA from cultured cells was isolated using QIAamp DNA Blood Mini kit (Qiagen). Two monkey cell lines, Vero and COS7, used in this study are derived from African green monkey. High molecular mass DNA was extracted by using a Blood and Cell Culture DNA Mini kit (Qiagen). Genomic DNAs of shrews, ground squirrels and the Gaboon viper were prepared from tissue samples using a phenol/chloroform extraction method or the Blood and Cell Culture DNA Mini kit. To minimize the risks of contamination, DNA extraction was performed in UV-irradiated safety cabinet with UV-irradiated pipettes, tubes and filter tips.

DNA samples. Genomic DNAs from chipmunks (*Tamias sibiricus*), Japanese giant flying squirrels (*Petaurista leucogenys*) and red and white giant flying squirrels (*Petaurista alborufus lena*) were obtained from the Department of Life Science and Agriculture, Obihiro University of Agriculture and Veterinary Medicine, Obihiro, Hokkaido, Japan.

Southern blot hybridization. Genomic DNA (5 μg) was digested with appropriate restriction endonucleases (TaKaRa). After electrophoresis in a 0.9% agarose gel, DNA was transferred onto positively charged Nylon membranes (Roche) and baked at 120 °C for 30 min. The membrane was prehybridized in DIG Easy Hyb (Roche) at 32 °C for 30 min. Human and TLS EBLN and BDV N probes were labelled by DIG-High Prime (Roche). Hybridization was performed in DIG Easy Hyb containing 25 ng ml^{-1} probe at 32 °C overnight. The membrane was washed twice with 2× SSC, 0.1% SDS at room temperature for 5 min, and then washed twice with 0.5× SSC, 0.1% SDS at 50 °C for 15 min. For chemiluminescence detection, Anti-DIG-alkaline phosphatase, Fab (Roche) and CDP-Star (Roche) were used according to the manufacturer's instructions. The low-stringency condition can theoretically detect sequences having at least 75% identity with each probe.

F-PERT assay. F-PERT (fluorescent product-enhanced reverse transcriptase) assay was performed as described previously[26]. Briefly, cells were lysed in disruption buffer (40 mM Tris-HCl, pH 8.1; 50 mM KCl; 20 mM dithiothreitol; 0.2% NP-40) and the protein concentration was measured. For the reverse transcription reaction, 1 μg of the cellular protein in 10 μl disruption buffer and an equal volume of 2× RT mix (100 mM KCl; 20 mM Tris-HCl pH 8.3; 11 mM $MgCl_2$; 1 mM dATP, dCTP, dGTP and dTTP; 0.4 μM reverse primer: 5′-CACAGGTCAAACCTCCTAG GAATG-3′, 0.2% NP-40; 20 mM dithiothreitol; 0.8 U μl^{-1} RNasin (Promega); 314 ng μl^{-1} calf thymus DNA (Sigma) and 1.5 ng MS2 RNA (Roche)) were mixed and incubated at 48 °C for 30 min. cDNA was mixed with forward primer: 5′-TCCTGCTCAACTTCCTGTCGAG-3′, reverse primer, probe: 5′-(FAM)-TC TTTAGCGAGACGCTACCATGGCTA-(TAMRA)-3′ and 2× TaqMan Universal PCR Master Mix (Applied Biosystems). Real-time PCR was carried out in an ABI 7900HT Fast Real-Time PCR System using the following parameters: 95 °C 10 min, then 50 cycles consisting of 94 °C for 30 s and 64 °C for 1 min. SuperScript III reverse transcriptase (Invitrogen) was used as standard control.

Virus infection. The BDV strains, huP2br, He/80 and recombinant BDV expressing GFP (rBDV-5′ GFP), were used in this study. Virus stock was prepared from the supernatants of BDV-infected cells. Confluent BDV-infected cells were washed with 20 mM HEPES, pH 7.5 and incubated with 5 ml of 20 mM HEPES (pH 7.5) containing 250 mM $MgCl_2$ and 1% FCS for 1.5 h at 37 °C. Supernatants were harvested and centrifuged at 2,500*g* for 5 min. The resulting supernatants were used for virus stock. The infectious titre was determined by focus forming assay as described previously[27]. The cell lines used in this study were cultured in Dulbecco's modified Eagle's medium (DMEM)-containing 10% fetal bovine serum (FBS). Newborn Balb/c mice (Oriental kobo) were inoculated intracranially with 200 focus forming units of BDV stock per animal within 24 h after birth. Infected animals were sacrificed at 21 days post-infection. The brains were collected for further analyses. All animal experiments conformed to the guide for the care and use of laboratory animals in the Research Institute for Microbial Diseases, Osaka University, Japan.

Alu-PCR analysis. Integration of BDV sequences into host genomes was detected by using primers specific to human Alu repeats and to BDV N region. First round amplification was performed in a final volume of 25 μl containing 0.5 U Ex Taq (TAKARA), 1× Ex Taq buffer, 0.2 mM dNTP, BDV N-specific primer, Alu primer and 100 ng of high molecular mass genome DNA. As control, PCR without the Alu primer was also performed. The condition of first PCR was as follows: denature for 5 min, 20 cycles of 94 °C for 30 s, 53 °C for 30 s, 72 °C for 4 min, followed by an extended elongation at 72 °C for 10 min. The second round PCR reaction was carried out with 1 μl of the first reaction using BDV N-specific nested primers. The reaction was run as follows: denature for 5 min, 40 cycles of 94 °C for 30 s, 60 °C for 30 s, 72 °C for 20 s with the final extension at 72 °C for 3 min. The sequence information for primers used in Alu-PCR is available on request.

Amplification of virus–host junction. Virus–host junctions were amplified by using Alu-PCR and inverse PCR methods. Alu-PCR analysis was performed as described previously[28]. Briefly, the first round PCR reaction was carried out with 100 ng of high molecular mass genome DNA in a final volume of 25 μl containing 0.5 U Ex Taq, 0.2 mM dNTP, 2 μM BDV-specific primer and 0.2 μM Alu primer under the following conditions: denaturing at 94 °C for 1 min, 10 cycles of 94 °C for 30 s, 59 °C for 30 s, 70 °C for 3 min, followed by an extended elongation at 70 °C for 10 min. After amplification, 0.5 U of uracil DNA glycosylase (New England Biolabs) was added into the tubes and incubated at 37 °C for 30 min. After heating at 94 °C for 10 min to break DNA strands at apurinic dUTP sites, the next amplification primers, Tag- and BDV-specific primers, were added. Second round PCR was performed as follows: after denaturing at 94 °C for 2 min, 20 cycles of touchdown PCR in which the annealing temperature was decreased one degree every other cycle from 65 °C to 56 °C. The remaining 20 cycles were run with the annealing temperature at 55 °C, followed by an extended elongation at 72 °C for 3 min. One microlitre of the second round PCR products was further amplified with Tag- and BDV-specific primers as follows: after denaturing for 2 min, 25 cycles of 94 °C for 30 s, 60 °C for 30 s, 72 °C for 3 min with the final extension at 72 °C for 3 min. Amplified DNA was electrophoresed, extracted and then sequenced.

Inverse PCR was described elsewhere[29]. Briefly, 1 μg genomic DNA was digested with an appropriate restriction enzyme, including ApaI, BamHI, EcoRI, NspI, PstI or XspI, for 3 h. Digested DNA was purified with QIAquick PCR Purification kit (Qiagen) and diluted with T4 DNA ligase buffer to a final DNA concentration of 1 ng μl^{-1}, and then T4 DNA ligase (New England Biolabs) was added to a final concentration of 4 U μl^{-1}. After ligation at 16 °C for 16 h, ligated DNA was isolated using a QIAquick PCR Purification kit. Five microlitres of the eluate were used for nested PCR. First round PCR was conducted in a 50 μl final volume containing 1 U TaKaRa Ex Taq, 0.2 mM dNTP and 0.2 μM BDV-specific primer set with the following program: after denaturing at 94 °C for 2 min, 20 cycles of 94 °C for 30 s, 70 °C for 30 s (temperature was decreased one degree every other cycle), 72 °C for 4 min and 20 cycles of 94 °C for 30 s, 60 °C for 30 s, 72 °C for 4 min with the final extension at 72 °C for 3 min. Second round PCR was performed with 1 μl of the first reaction. The reaction condition was 94 °C for 2 min, 25 cycles of 94 °C for 30 s, 58 °C for 30 s, 72 °C for 4 min with the final extension at 72 °C for 3 min. PCR products were electrophoresed and DNA was extracted from the desired bands and sequenced. Sequence information for primers used in this study is available on request.

26. Lovatt, A. *et al.* High throughput detection of retrovirus-associated reverse transcriptase using an improved fluorescent product enhanced reverse transcriptase assay and its comparison to conventional detection methods. *J. Virol. Methods* **82**, 185–200 (1999).
27. Ohtaki, N. *et al.* Downregulation of an astrocyte-derived inflammatory protein, S100B, reduces vascular inflammatory responses in brains persistently infected with Borna disease virus. *J. Virol.* **81**, 5940–5948 (2007).
28. Minami, M., Poussin, K., Brechot, C. & Paterlini, P. A novel PCR technique using Alu-specific primers to identify unknown flanking sequences from the human genome. *Genomics* **29**, 403–408 (1995).
29. Wo, Y. Y., Peng, S. H. & Pan, F. M. Enrichment of circularized target DNA by inverse polymerase chain reaction. *Anal. Biochem.* **358**, 149–151 (2006).

©2010 Macmillan Publishers Limited. All rights reserved

Mutsuo Yamaya, Hidekazu Nishimura, Kyoko Shinya, Yukimasa Hatachi, Takahiko Sasaki, Hiroyasu Yasuda, Motoki Yoshida, Masanori Asada, Naoya Fujino, Takaya Suzuki, Xue Deng, Hiroshi Kubo and Ryoichi Nagatomi
Am J Physiol Lung Cell Mol Physiol 299:160-168, 2010. First published Jun 11, 2010;
doi:10.1152/ajplung.00376.2009

You might find this additional information useful...

This article cites 38 articles, 18 of which you can access free at:
http://ajplung.physiology.org/cgi/content/full/299/2/L160#BIBL

Updated information and services including high-resolution figures, can be found at:
http://ajplung.physiology.org/cgi/content/full/299/2/L160

Additional material and information about ***AJP - Lung Cellular and Molecular Physiology*** can be found at:
http://www.the-aps.org/publications/ajplung

This information is current as of August 2, 2010 .

AJP - Lung Cellular and Molecular Physiology publishes original research covering the broad scope of molecular, cellular, and integrative aspects of normal and abnormal function of cells and components of the respiratory system. It is published 12 times a year (monthly) by the American Physiological Society, 9650 Rockville Pike, Bethesda MD 20814-3991. Copyright © 2010 by the American Physiological Society. ISSN: 1040-0605, ESSN: 1522-1504. Visit our website at http://www.the-aps.org/.

Downloaded from ajplung.physiology.org on August 2, 2010

Am J Physiol Lung Cell Mol Physiol 299: L160–L168, 2010.
First published June 11, 2010; doi:10.1152/ajplung.00376.2009.

TRANSLATIONAL PHYSIOLOGY

Inhibitory effects of carbocisteine on type A seasonal influenza virus infection in human airway epithelial cells

Mutsuo Yamaya,[1] Hidekazu Nishimura,[2] Kyoko Shinya,[3] Yukimasa Hatachi,[4] Takahiko Sasaki,[5] Hiroyasu Yasuda,[6] Motoki Yoshida,[7] Masanori Asada,[7] Naoya Fujino,[1] Takaya Suzuki,[1] Xue Deng,[6] Hiroshi Kubo,[1] and Ryoichi Nagatomi[8]

[1]Department of Advanced Preventive Medicine for Infectious Disease, Tohoku University School of Medicine, and [2]Virus Research Center, Clinical Research Division, Sendai National Hospital, Sendai; [3]Division of Zoonosis, Department of Microbiology and Infectious Diseases, Graduate School of Medicine, Kobe University, Kobe; [4]Department of Respiratory Medicine, Graduate School of Medicine Kyoto University, Kyoto; and Departments of [5]Respiratory Medicine and [6]Innovation of New Biomedical Engineering Center, Tohoku University School of Medicine, [7]Department of Geriatrics and Gerontology, Tohoku University Hospital, and [8]Medicine and Science in Sports and Exercise, Tohoku University School of Medicine, Sendai, Japan

Submitted 26 October 2009; accepted in final form 6 June 2010

Yamaya M, Nishimura H, Shinya K, Hatachi Y, Sasaki T, Yasuda H, Yoshida M, Asada M, Fujino N, Suzuki T, Deng X, Kubo H, Nagatomi R. Inhibitory effects of carbocisteine on type A seasonal influenza virus infection in human airway epithelial cells. *Am J Physiol Lung Cell Mol Physiol* 299: L160–L168, 2010. First published June 11, 2010; doi:10.1152/ajplung.00376.2009.—Type A human seasonal influenza (FluA) virus infection causes exacerbations of bronchial asthma and chronic obstructive pulmonary disease (COPD). L-carbocisteine, a mucolytic agent, reduces the frequency of common colds and exacerbations in COPD. However, the inhibitory effects of L-carbocisteine on FluA virus infection are uncertain. We studied the effects of L-carbocisteine on FluA virus infection in airway epithelial cells. Human tracheal epithelial cells were pretreated with L-carbocisteine and infected with FluA virus (H_3N_2). Viral titers in supernatant fluids, RNA of FluA virus in the cells, and concentrations of proinflammatory cytokines in supernatant fluids, including IL-6, increased with time after infection. L-carbocisteine reduced viral titers in supernatant fluids, RNA of FluA virus in the cells, the susceptibility to FluA virus infection, and concentrations of cytokines induced by virus infection. The epithelial cells expressed sialic acid with an α2,6-linkage (SAα2,6Gal), a receptor for human influenza virus on the cells, and L-carbocisteine reduced the expression of SAα2,6Gal. L-carbocisteine reduced the number of acidic endosomes from which FluA viral RNA enters into the cytoplasm and reduced the fluorescence intensity from acidic endosomes. Furthermore, L-carbocisteine reduced NF-κB proteins including p50 and p65 in the nuclear extracts of the cells. These findings suggest that L-carbocisteine may inhibit FluA virus infection, partly through the reduced expression of the receptor for human influenza virus in the human airway epithelial cells via the inhibition of NF-κB and through increasing pH in endosomes. L-carbocisteine may reduce airway inflammation in influenza virus infection.

SAα2,6Gal; bronchial asthma; chronic obstructive pulmonary disease

MUCOLYTIC AGENTS INCLUDING *N*-acetylcysteine, L-carbocisteine, and ambroxol have various physiological functions such as antioxidant effects (39), reduction of mucin 5AC protein production (27), and improvement of airway mucociliary transport (20). Mucolytic agents are also suggested to have clinical benefits in reducing the frequency of exacerbations and improvement of quality of life in patients with chronic obstructive pulmonary disease (COPD) (40).

Exacerbations of COPD have been reported to be caused by viral and bacterial infection (22) as well as by exposure to oxidants in airways. Of the viruses, type A seasonal influenza (FluA) is one of the pathogens that cause COPD exacerbations especially in the winter season (19). Influenza vaccine reduces the mortality rate in COPD patients in the winter season (14) and is recommended in the management of COPD patients in stable conditions. The clinically used anti-influenza drugs, which include neuraminidase inhibitors such as oseltamivir and zanamivir, and M_2 ion channel blockers such as amantadine, are beneficial for human influenza infection (1). On the other hand, a mucolytic agent, L-carbocisteine, reduces the frequency of common colds as well as the frequency of exacerbations in COPD patients (36, 40). Yang et al. (35) demonstrated that a mucolytic agent, ambroxol, inhibits influenza-virus proliferation in the mouse airway. Likewise, L-carbocisteine inhibits the infection of rhinovirus (37), a major cause of COPD exacerbations. However, the effects of L-carbocisteine on influenza virus infection have not been studied.

In an infection of FluA virus, the viruses are attached to sialic acid (SAα2,6Gal), a receptor for human influenza virus, on airway epithelial cells (18). The viruses are then delivered into the cytoplasm, and the RNA of the viruses is released from acidic endosomes into the cytoplasm of the cells (17). As we demonstrated, L-carbocisteine reduces the number of acidic endosomes in human tracheal epithelial cells (37). However, the effects of L-carbocisteine on FluA virus infection are still uncertain.

Influenza virus infection induces airway inflammation through the production of proinflammatory cytokines and chemokines such as IL-6, IL-8, and IFN-γ-inducible protein (IP)-10 (7, 30) and through the epithelial cell damage, both of which are associated with exacerbations of COPD (12). L-

Address for reprint requests and other correspondence: M. Yamaya, Dept. of Advanced Preventive Medicine for Infectious Disease, Tohoku Univ. School of Medicine, Seiryo-machi, Aoba-ku, Sendai, 980-8575, Japan (e-mail: myamaya@m.tains.tohoku.ac.jp).

1040-0605/10 Copyright © 2010 the American Physiological Society

Downloaded from ajplung.physiology.org on August 2, 2010

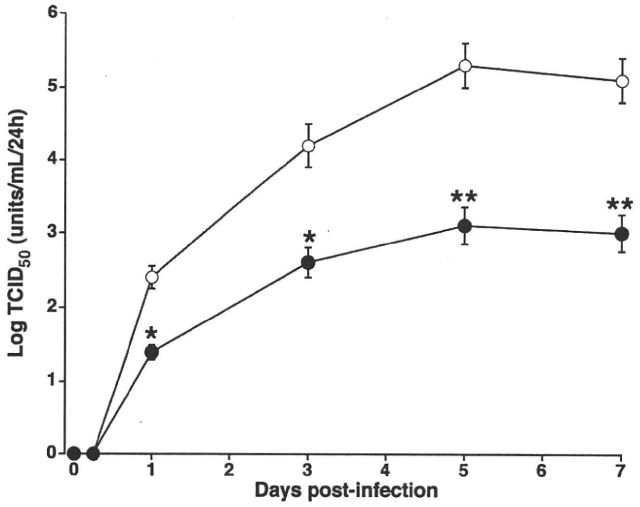

Fig. 1. The time course of viral release in supernatant fluids of human tracheal epithelial cells obtained at different times after exposure to 0.5×10^{-3} tissue culture infective dose ($TCID_{50}$) U/cell type A human seasonal influenza (FluA) virus in the presence of L-carbocisteine (10 μM; ●) or vehicle of L-carbocisteine (0.1% double-distilled water; ○). The rates of change in FluA virus concentration in the supernatant fluids are expressed as $TCID_{50}$ U/ml/24 h. Results are means ± SE from 5 different tracheae. Significant differences from viral infection alone are indicated by $*P < 0.05$ and $**P < 0.01$.

carbocisteine reduces the production of proinflammatory cytokines after rhinovirus infection (37), whereas the inhibitory effects of L-carbocisteine on the production of proinflammatory cytokines by FluA virus infection are uncertain.

In the present study, we studied the effects of L-carbocisteine on FluA virus infection in cultured human tracheal epithelial cells that are targets of the viruses. We also examined the effects of L-carbocisteine on the expression of SAα2,6Gal, a receptor for human influenza virus, and on acidic endosomes to examine the inhibitory mechanisms.

MATERIALS AND METHODS

Media components. Reagents for cell culture media were obtained as follows: DMEM, Ham's F-12 medium, and FCS were from GIBCO BRL Life Technologies (Palo Alto, CA); PBS, MEM, and trypsin were from Sigma (St. Louis, MO); and Ultroser G (USG) was from Pall BioSepra (Cergy-Saint-Christophe, France).

Human tracheal epithelial cell culture. Isolation and culture of the human tracheal surface epithelial cells were performed as described previously (29, 34). The human tracheal surface epithelial cells were plated at 5×10^5 viable cells/ml in plastic tubes with round bottoms (16-mm diameter and 125-mm length; Becton Dickinson) coated with human placental collagen because attachment of the cells in plastic tubes was much better than that in glass tubes (data not shown) (34). Cells were cultured in 1 ml of a mixture of DMEM/Ham's F-12 (DF-12) medium (50:50 vol/vol) containing 2% USG and antibiotics (29, 34). The tubes were laid with a slant of ~5° and kept stationary, and cells were immersed in 1 ml of medium and cultured at 37°C in 5% CO_2-95% air in a humid incubator (29, 34). Because of this laid position of the plastic tubes, the cells attached and proliferated on the inner surface of the lateral wall of the tubes and the round shape of the bottom of the tubes. The surface area of culture vessels of the plastic tubes covered by the cells became 11.7 ± 0.2 cm^2 ($n = 3$). Cells in the tubes were cultured at 37°C in 5% CO_2-95% air. We confirmed the presence of a dome formation when the cells made confluent cell sheets on *days 5–7* of culture using an inverted microscope (MIT-2; Olympus, Tokyo, Japan) (29) as described by Widdicombe et al. (32).

Tracheas for cell cultures were obtained after death from 36 patients (age, 71 ± 4 yr; 12 female, 24 male) without complications with bronchial asthma. Five patients were complicated with COPD. The causes of death included malignant tumor other than lung cancer ($n = 17$), acute myocardial infarction ($n = 5$), renal failure ($n = 3$), congestive heart failure ($n = 3$), cerebral bleeding ($n = 2$), rupture of an aortic aneurysm ($n = 2$), cerebral infarction ($n = 1$), sepsis ($n = 1$), mitral stenosis ($n = 1$), and malignant lymphoma ($n = 1$). Of 36 patients, 15 were exsmokers, and 21 had never smoked. This study was approved by the Tohoku University Ethics Committee.

Culture of Madin-Darby canine kidney cells. Madin-Darby canine kidney (MDCK) cells were cultured in T-25 flasks (Becton Dickinson) in MEM containing 10% FCS supplemented with 5×10^4 U/l penicillin and 50 mg/l streptomycin (15). The cells were then plated in plastic dishes (96-well plate; Becton Dickinson) or in plastic tubes with round bottoms (16-mm diameter and 125-mm length; Becton Dickinson). Cells in the plastic dishes or tubes were cultured at 37°C in 5% CO_2-95% air.

Viral stocks. FluA virus (H_3N_2) was prepared in our laboratory from a patient complaining of fever and rhinorrhea (15). FluA virus was identified by the hemadsorption inhibition (HI) test using an antiserum (New York/55/2004) as described previously (15). To generate stocks of FluA virus, MDCK cells in plastic tubes were cultured in the medium (1.1 ml) containing 100 μl of FluA virus stock solution [1.0×10^3 50% tissue culture infective dose ($TCID_{50}$) units in 100 μl] and 1 ml of MEM supplemented with 5×10^4 U/l penicillin, 50 mg/l streptomycin, and 3.5 μg/ml trypsin. Cells in the plastic tubes were cultured at 33°C in 5% CO_2-95% air (15). To obtain the FluA virus solution, 7 days after infection with FluA virus, cells and medium were frozen by immersing the tubes in ethanol at −80°C, thawed, and sonicated. The virus-containing fluid was frozen in aliquots at −80°C.

Detection and titration of influenza viruses. Detection and titration of influenza viruses in supernatant fluids was performed with the

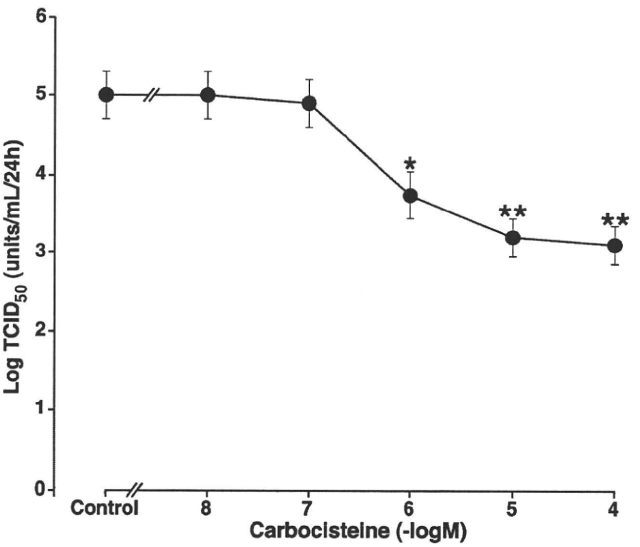

Fig. 2. Concentration-response effects of L-carbocisteine on the viral release in supernatant fluids collected during 3 days (72 h) to 5 days (120 h) after infection. The cells were treated with L-carbocisteine or vehicle (Control; 0.1% double-distilled water) from 3 days before FluA virus infection until the end of the experiments after FluA virus infection. The rates of change in FluA virus concentration in the supernatant fluids are expressed as $TCID_{50}$ U/ml/24 h. Results are means ± SE from 7 different tracheae. Significant differences from vehicle alone (Control) are indicated by $*P < 0.05$ and $**P < 0.01$.

Downloaded from ajplung.physiology.org on August 2, 2010

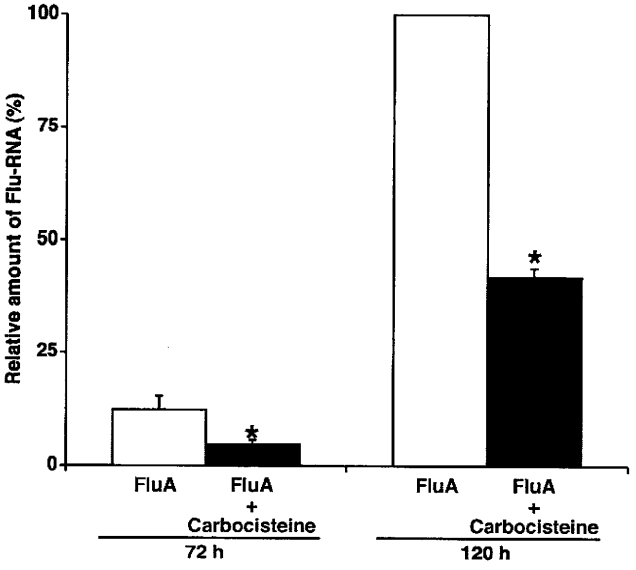

Fig. 3. Replication of FluA viral RNA in human tracheal epithelial cells 3 days (72 h) and 5 days (120 h) after infections of FluA virus in the presence of L-carbocisteine (10 μM; FluA + Carbocisteine) or double-distilled water (0.1%) as a vehicle (control; FluA) as detected by real-time quantitative RT-PCR. Results are expressed as relative amount of RNA expression (%) compared with those of maximal FluA viral RNA at *day 5* (120 h) in the cells treated with vehicle and reported as means ± SE from 5 samples. Significant differences from treatment with a vehicle (FluA) at each time are indicated by $*P < 0.05$.

endpoint method (5) by infecting replicate confluent MDCK cells in plastic 96-well dishes with serial 10-fold dilutions of virus-containing supernatant fluids as previously described (15, 34). In brief, virus-containing supernatant fluids were 10-fold diluted in MEM supplemented with 5×10^4 U/l penicillin, 50 mg/l streptomycin, and 3.5 μg/ml trypsin (15) and added into the replicate MDCK cells in the wells (200 μl/well) of 96-well dishes. MDCK cells in the wells were then cultured at 33°C in 5% CO_2-95% air for 7 days, and the presence of the typical cytopathic effects (CPE) of influenza virus was examined in all replicate cells as described previously (5, 15). The number of wells that showed CPE of influenza was counted in each dilution of supernatant fluids. Then, the dilution of virus-containing supernatant fluids, which showed CPE in >50% of replicate wells, and the dilution of the fluids, which showed CPE in <50% of replicate wells, were estimated. Based on these data, $TCID_{50}$ was calculated with the method as previously described (5). Because the human tracheal epithelial cells were cultured in 1 ml of DF-12 medium containing 2% USG in the tubes, viral titers in supernatant fluids are expressed as $TCID_{50}$ U/ml (5, 15, 34). Furthermore, the rates were obtained by dividing the value of influenza titer ($TCID_{50}$ U/ml) in supernatant fluids by incubation time and are expressed as $TCID_{50}$ U/ml/24 h (34).

Viral infection of the cells. Infection of FluA virus to human tracheal epithelial cells was performed with methods previously described (29, 34) with some modification. A stock solution of influenza virus (H_3N_2, New York/55/2004, 100 μl in each tube, 1.0×10^4 $TCID_{50}$ U/ml) was added to the cells in the tubes. Because the number of the epithelial cells in the tubes was $2.0 \pm 0.3 \times 10^6$ cells/tube ($n = 7$), the multiplicity of infection (MOI) was 0.5×10^{-3} $TCID_{50}$ U/cell. We found in preliminary experiments that the human tracheal epithelial cells detached from culture vessels of the tubes after FluA virus infection when the cells were infected with at least 0.5×10^{-2} $TCID_{50}$ U/cell FluA virus, and thus the cells were infected with 0.5×10^{-3} $TCID_{50}$ U/cell viruses. After a 1-h incubation at 33°C in 5% CO_2-95% air (15, 29, 34), the FluA viral solution was removed, and the cells were rinsed one time with 1 ml of PBS. The cells were then fed with 1 ml of fresh DF-12 medium containing 2% USG supplemented with antibiotics. The tubes were laid with a slant of ~5° and kept stationary in a humid incubator, and cells were cultured at 33°C in 5% CO_2-95% air as described previously (29, 34). The supernatant fluids were stored at −80°C for the determination of viral titers and cytokine concentrations.

Treatment with L-carbocisteine. The cultured human tracheal epithelial cells were treated with L-carbocisteine (10 μM) from 3 days before FluA virus infection until the end of the experiments after FluA virus infection (34, 37) unless we describe other concentrations or treatment periods. The concentrations of L-carbocisteine (10 μM) were chosen because the maximum concentrations of L-carbocisteine in the serum became >10 μM after oral ingestion of 1,500 mg of L-carbocisteine (9).

To examine the concentration-dependent effects of L-carbocisteine on FluA virus infection, cells were treated with L-carbocisteine at concentrations ranging from 10 nM to 100 μM.

Collection of supernatant fluids for measurements. We measured the time course of the release of FluA virus and proinflammatory cytokines with methods previously described (29, 34) with some modifications. In brief, to measure the release of FluA virus and proinflammatory cytokines during the first hour after virus infection, we collected the supernatant fluids at 1 h after FluA virus infection. After collecting supernatant fluids at 1 h after infection, the cells were rinsed with PBS, and 1 ml of DF-12 medium containing 2% USG was replaced. Furthermore, to measure the release of FluA virus and proinflammatory cytokines from 1 h to 1 day after FluA virus infection, we collected supernatant fluids at 1 day (24 h) after virus infection. To measure the release of FluA virus and proinflammatory cytokines during 1–3 days after virus infection, supernatant fluids were collected at 1 day after infection, the cells were rinsed with PBS, and 1 ml of DF-12 medium containing 2% USG was replaced. Supernatant fluids were also collected at 3 days after infection. Likewise, to measure the release of FluA virus and proinflammatory cytokines during 3–5 days after FluA virus infection, after collecting supernatant fluids at 3 days after infection, the cells were rinsed with

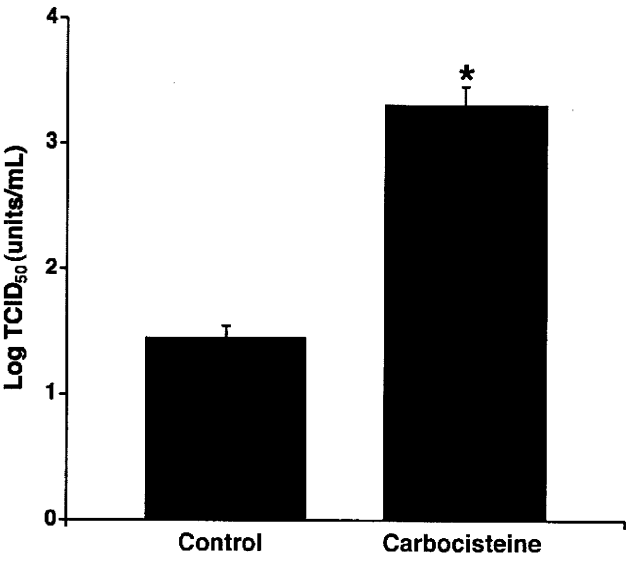

Fig. 4. The minimum dose of FluA virus necessary to cause infection in human tracheal epithelial cells treated with either L-carbocisteine (10 μM, 3 days; Carbocisteine) or vehicle (Control; 0.1% double-distilled water). The minimum dose of FluA virus necessary to cause infection is expressed as $TCID_{50}$ U/ml. Results are means ± SE from 7 different tracheae. Significant differences from vehicle alone (Control) are indicated by $*P < 0.05$.

Downloaded from ajplung.physiology.org on August 2, 2010

PBS, and 1 ml of fresh medium was replaced. Supernatant fluids were also collected at 5 days after virus infection. The cells were then rinsed with PBS, and 1 ml of fresh medium was replaced. Supernatant fluids were also collected at 7 days after infection to measure the release of FluA virus and proinflammatory cytokines during 5–7 days after FluA virus infection.

To measure the concentrations of proinflammatory cytokines before FluA infection, supernatant fluids were also collected just before FluA infection.

Effects of L-carbocisteine on susceptibility to influenza virus infection. The effects of L-carbocisteine on the susceptibility to influenza virus infection were evaluated as previously described (26, 29, 34) using epithelial cells pretreated with L-carbocisteine (10 μM) or vehicle (0.1% double-distilled water) from 3 days before infection with FluA virus until just finishing the virus infection. The epithelial cells were then exposed to serial 10-fold dilutions of FluA virus (H_3N_2) or vehicle of influenza virus (MEM containing 3.5 μg/ml trypsin) for 1 h at 33°C in 5% CO_2-95% air. Because we found in the preliminary experiments that the maximum virus titers were observed in the supernatant fluids collected for 3–5 days, the presence of FluA virus was determined in the supernatant fluids collected for 3–5 days after infection with methods described above to assess whether infection occurred at each dose of influenza virus used.

Quantification of influenza virus RNA. To quantify FluA (H_3N_2) virus RNA and ribosomal RNA (rRNA) expression in the human tracheal epithelial cells after virus infection, real-time quantitative RT-PCR using the *Taq*Man technique (Roche Molecular Diagnostics) was performed as previously described (34) with some modification. Each RNA sample (100 ng/10 μl water) was mixed in 40 μl of buffer containing 100 nM forward primer (5′-AGATGAGTCTTCTAACCGAGGTCG-3′), 100 nM reverse primer (5′-TGCAAAAAACATCTTCAAGTCTCTG-3′), and other reagents as previously described (25). The *Taq*Man probe influenza virus [5′-(FAM) TCAGGCCCCCTCAAAGCCGA (TAMRA)-3′] was designed for FluA virus (25). The fragment of RNA extracted from the human tracheal epithelial cells at 3 days (72 h) or at 5 days (120 h) after infection by FluA virus was reverse-transcribed into cDNA (30 min at 48°C) and amplified by PCR for 40 cycles (15 s at 95°C and 1 min at 60°C). The standard curve was obtained between the fluorescence emission signals and cycle threshold (C_T) by means of 10-fold dilutions of the total RNA, extracted from 1.0×10^4 $TCID_{50}$ U/ml FluA virus in the supernatant fluids of the MDCK cells 7 days after infection with FluA virus (0.5×10^{-3} $TCID_{50}$ U/cell). Real-time quantitative RT-PCR for rRNA was also performed using the same PCR products. The standard curve was obtained between the fluorescence emission signals and C_T by means of 10-fold dilutions of the RNA extracted from the cells. The expression of FluA virus RNA was normalized to the constitutive expression of rRNA.

Detection of SAα2,6Gal in human tracheal epithelial cells. SAα2,6Gal in human tracheal epithelial cells was detected using lectins as previously described (23). In brief, human tracheal epithelial cells were cultured for 7 days on a filter membrane (0.45-μm pore size and 0.6-cm^2 area; Millicell-CM inserts; Millipore Products Division) coated with collagen gel (PureCol; Inamed) as described previously (33). Because cells were cultured with air-interface methods (33), culture medium was supplied from the basolateral side of the cell

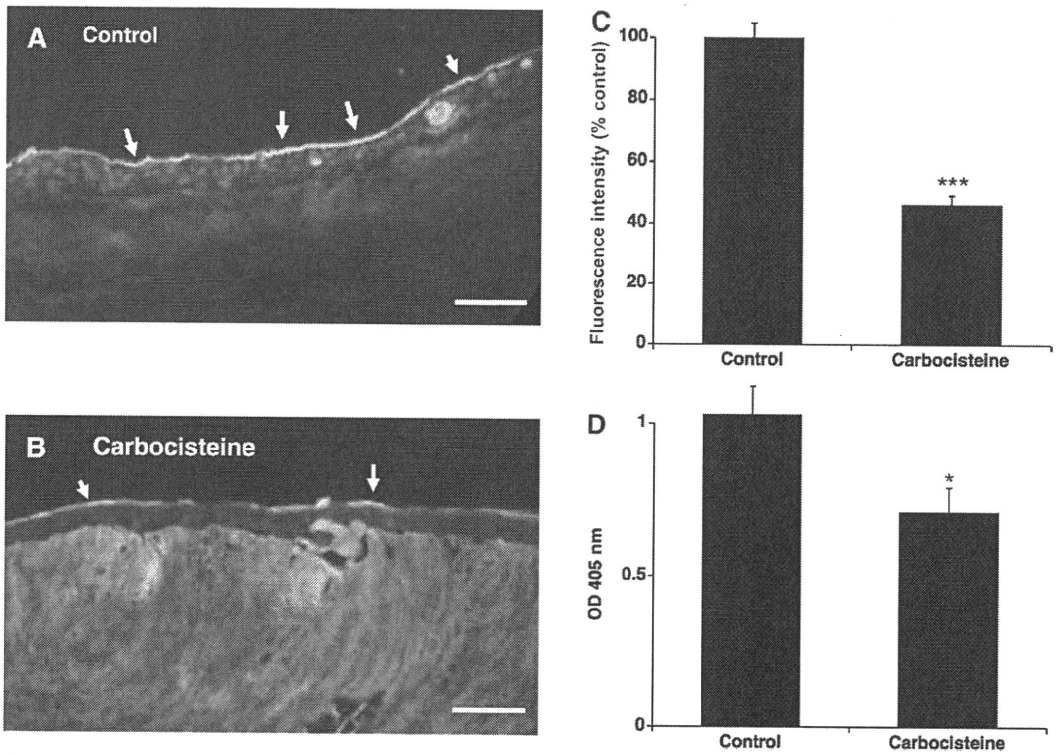

Fig. 5. *A* and *B*: the expression of SAα2,6Gal (arrows), a receptor for human influenza virus, on the cultured human tracheal epithelial cells treated with L-carbocisteine (10 μM, 72 h; Carbocisteine) or vehicle of L-carbocisteine (0.1% double-distilled water, 72 h; Control). Data are representative of 8 different experiments. Bar = 100 μm. *C*: the fluorescence intensity of SAα2,6Gal on the mucosal surface of the human tracheal epithelial cells treated with L-carbocisteine (10 μM, 72 h; Carbocisteine) or vehicle of L-carbocisteine (0.1% double-distilled water, 72 h; Control). Results are expressed as relative fluorescence intensity (%) compared with that treated with vehicle and reported as means ± SE from 8 samples. Significant differences from control values are indicated by $***P < 0.001$. *D*: concentrations of SAα2,6Gal measured with enzyme-linked lectin assay (ELLA) in the cells treated with L-carbocisteine (10 μM, 72 h; Carbocisteine) or vehicle of L-carbocisteine (0.1% double-distilled water, 72 h; Control). Results are expressed as optical density (OD) and are means ± SE from 5 different tracheae. Significant differences from vehicle alone (Control) are indicated by $*P < 0.05$.

Downloaded from ajplung.physiology.org on August 2, 2010

sheets through the filter membrane. Then, the cells were treated with L-carbocisteine (10 μM) for 3 days and fixed in 10% paraformaldehyde.

To study the expression of SAα2,6Gal in human tracheal epithelial cells, paraffin-embedded cell sheets were cut into 5-μm thick sections with a microtome and mounted on 3-aminopropyltriethoxysilane-coated slides (Matsunami Glass Industries, Tokyo, Japan). Sections were incubated with 250 μl of FITC-labeled *Sambucus nigra* (SNA) lectin (1:100; Vector Laboratories, Burlingame, CA) overnight at 4°C. Sections were incubated with Alexa Fluor 594-conjugated streptavidin (1:250; Molecular Probes, Eugene, OR) for 2 h at room temperature and counterstained with 4′,6′-diamidino-2-phenylindole (DAPI; Dojindo Molecular Technologies, Kumamoto, Japan). The cover glasses were mounted on the sections and observed with a fluorescence microscope (BZ-8000; Keyence, Osaka, Japan). The excitation wavelengths were 470 nm (FITC), 560 nm (Alexa Fluor 594), and 360 nm (DAPI), and the emitted light from the cells was detected through 495-, 595-, and 400-nm filters, respectively. The fluorescence intensity was calculated using a fluorescence image analyzer system (Lumina Vision; Mitani, Fukui, Japan) equipped with a fluorescence microscope.

We also measured the amounts of SAα2,6Gal in the cells with enzyme-linked lectin assay (ELLA) (11, 21) with some modification. SAα2,6Gal in the cells was extracted using Glycoprotein Isolation Kits (Thermo Scientific). The extracted samples were diluted to concentrations of 15 μg/ml with Coating Solution Concentrate (KPL), and diluted samples were coated on Costar ELISA plates in triplicate overnight at 4°C. The plate was washed four times with TBS and then blocked for 1 h with freshly made TBS-Tween 20. Plates were then incubated for 2 h with biotinylated SNA (diluted 1:200), washed four times with TBS-Tween 20, and then incubated at room temperature with alkaline phosphatase-conjugated streptavidin at 1:1,000 dilution for 1 h. Plates were developed with alkaline phosphatase substrate for 15 min. Absorption readings were taken at 405 nm, and results are expressed as optical density (OD).

Measurement of changes in acidic endosomes. The distribution and the fluorescence intensity of acidic endosomes in the cells were measured as previously described with a dye, LysoSensor DND-189 (Molecular Probes) (29, 34). Because the cells were pretreated with L-carbocisteine for 3 days before FluA virus infection, we studied the effects of a 3-day treatment of L-carbocisteine (10 μM) on the distribution and the fluorescence intensity of acidic endosomes. Because each cell contains many acidic endosomes, we measured the average fluorescence intensity from many acidic endosomes in each cell. We measured the average fluorescence intensity for each cell in 100 human tracheal epithelial cells and calculated the mean value of fluorescence intensity of the cell sheets observed. The mean value of fluorescence intensity of the cell sheets treated with L-carbocisteine (10 μM) was expressed as percentage of control value compared with the fluorescence intensity of the cell sheets treated with vehicle of L-carbocisteine (0.1% double-distilled water).

Measurement of cytokine production. We measured IL-1β, IL-6, and IL-8 of supernatant fluids by specific ELISAs (29, 34). To demonstrate the time course of cytokines release, we expressed the rates of change in cytokine concentration in the supernatant fluids. The rates were obtained by dividing the value of cytokine concentration in supernatant fluids by incubation time and are expressed as pg/ml/24 h.

NF-κB assay. Nuclear extracts from human tracheal epithelial cells were prepared by using a TransAM NF-κB p50, p52, p65, and Family Kit (Activ Motif) according to the manufacturer's instructions. After

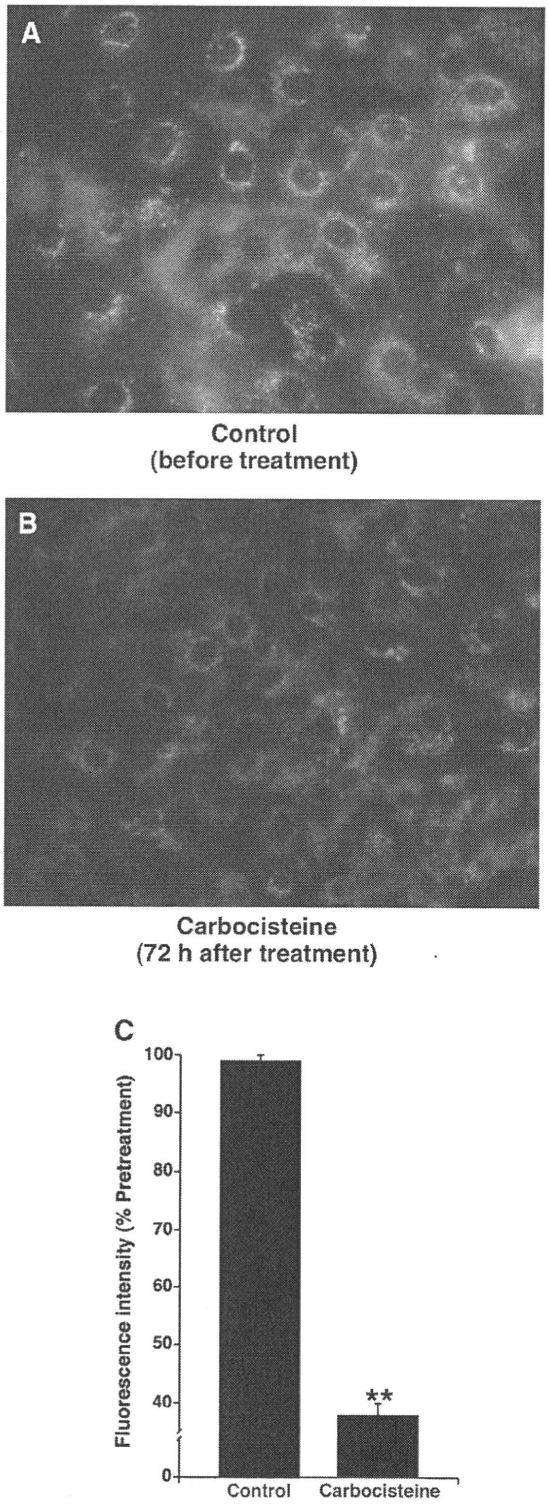

Fig. 6. *A* and *B*: changes in the distribution of acidic endosomes with green fluorescence in the human tracheal epithelial cells 3 days (72 h) after treatment with L-carbocisteine (10 μM; *B*) or vehicle of L-carbocisteine (0.1% double-distilled water; *A*). Data are representative of 5 different experiments. *C*: the fluorescence intensity of acidic endosomes 3 days (72 h) after treatment with L-carbocisteine (Carbocisteine; 10 μM) or vehicle of L-carbocisteine (Control; 0.1% double-distilled water). Results are means ± SE from 5 different tracheae. Significant differences from control values are indicated by $^{**}P < 0.01$.

Downloaded from ajplung.physiology.org on August 2, 2010

centrifugation at 20,000 *g* for 5 min at 4°C, nuclear extracts were assayed for p50, p65, c-Rel, p52, and RelB content. An equal amount of nuclear lysates was added to incubation wells precoated with the DNA-binding consensus sequence. The presence of subunits including translocated p50, p65, c-Rel, p52, and RelB was assayed by using a TransFactor Family Colorimetric Kit-NF-κB (BD Biosciences/Clontech) according to the manufacturer's instructions (10). Plates were read at 655 nm, and results are expressed as OD.

Statistical analysis. Results are expressed as means ± SE. Statistical analysis was performed using one-way measures of ANOVA. Subsequent post hoc analysis was made using Bonferroni method. For all analyses, values of $P < 0.05$ were assumed to be significant. In the experiments using culture of human tracheal epithelial cells, *n* refers to the number of donors (tracheae) from which cultured epithelial cells were used.

RESULTS

Effects of L-carbocisteine on influenza virus infection. Exposing confluent human tracheal epithelial cell monolayers to FluA virus (H_3N_2, 0.5×10^{-3} $TCID_{50}$ U/cell) consistently led to infection. No detectable virus was revealed at 1 h after infection, whereas FluA virus was detected in culture medium at 24 h, and the viral content progressively increased between 1 and 24 h after infection (Fig. 1). Evidence of continuous viral production was obtained by demonstrating that each of the supernatant fluids collected during 1–3, 3–5, and 5–7 days after infection contained significant levels of influenza virus (Fig. 1). The viral titer levels in supernatant fluids increased significantly with time for the first 5 days ($P < 0.05$ by ANOVA). Treatment of the cells with L-carbocisteine (10 μM) significantly decreased the viral titers of FluA virus in supernatant fluids from 24 h after infection (Fig. 1). FluA virus titer levels in supernatant fluids of the cells from 15 exsmokers did not differ from those from 21 patients who had never smoked (data not shown). Likewise, FluA virus titer levels in supernatant fluids of the cells from 5 patients complicated with COPD (5.5 ± 1.1 log $TCID_{50}$ U/ml/24 h, means ± SE; $P > 0.20$) did not differ from those from 31 patients without COPD (5.2 ± 0.9 log $TCID_{50}$ U/ml/24 h). No virus was detected in supernatant fluids after infection of UV-inactivated influenza virus (data not shown).

L-carbocisteine inhibited influenza virus infection concentration-dependently, and the maximum effect was obtained at 100 μM (Fig. 2).

Effects of L-carbocisteine on viral RNA by PCR. Further evidence of the inhibitory effects of L-carbocisteine on FluA viral RNA replication in human tracheal epithelial cells was provided by real-time quantitative RT-PCR analysis. The RNA extraction was performed at 3 days (72 h) and 5 days (120 h) after virus infection. FluA viral RNA replication in the cells was consistently observed at 3 days after infection and increased between 3 and 5 days after infection (Fig. 3). L-carbocisteine (10 μM) decreased the FluA viral RNA at 3 and 5 days after infection (Fig. 3).

Effects of L-carbocisteine on susceptibility to influenza virus infection. Treatment of the cells with L-carbocisteine (10 μM) decreased the susceptibility of the cells to infection by FluA

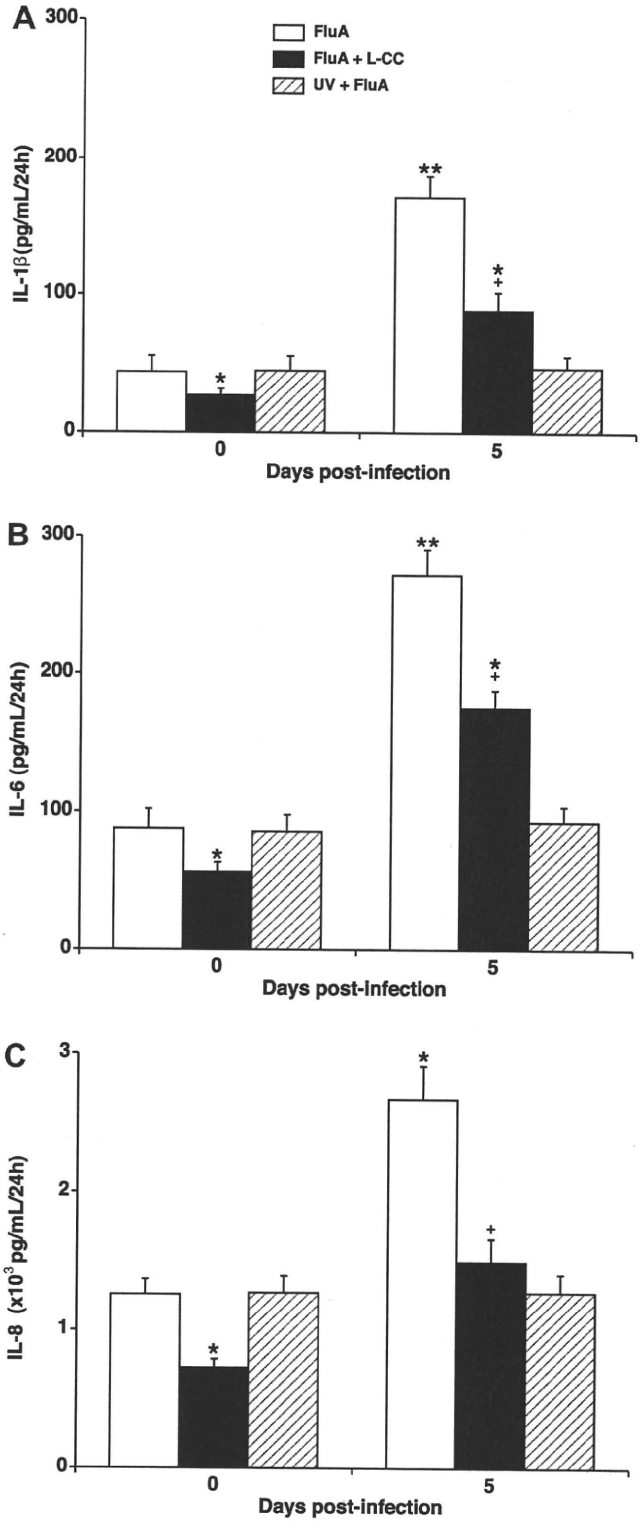

Fig. 7. *A–C*: the release of cytokines into supernatant fluids of human tracheal epithelial cells before and 5 days after FluA virus infection in the presence of L-carbocisteine (FluA + L-CC; 10 μM) or vehicle of L-carbocisteine (0.1% double-distilled water; FluA) and after UV-inactivated influenza virus infection (UV + FluA). The rates of change in cytokine concentration in the supernatant fluids are expressed as pg/ml/24 h. Results are means ± SE from 5 different tracheae. Significant differences from values before FluA virus infection (*time 0*) in the presence of vehicle are indicated by $^*P < 0.05$ and $^{**}P < 0.01$. Significant differences from FluA virus infection alone (FluA) 5 days after infection are indicated by $+P < 0.05$.

Downloaded from ajplung.physiology.org on August 2, 2010

virus (H_3N_2). The minimum dose of influenza virus necessary to cause infection in the cells treated with L-carbocisteine (10 μM, 3 days; 3.2 ± 0.3 log $TCID_{50}$ U/ml, $n = 5$; $P < 0.05$) was significantly higher than that in the cells treated with vehicle of L-carbocisteine (0.1% double-distilled water; 1.4 ± 0.2 log $TCID_{50}$ U/ml, $n = 5$; Fig. 4).

Effects of L-carbocisteine on SAα2,6Gal expression. SAα2,6Gal, a receptor for human influenza virus, was observed as green lines or spots on the mucosal surface of cultured human tracheal epithelial cell sheets (Fig. 5*A*). L-carbocisteine (10 μM, 72 h) reduced the number of green lines or spots on the cell sheets (Fig. 5*B*) and the fluorescence intensity from the receptor (by 54 ± 8% compared with that in vehicle of L-carbocisteine; $P < 0.001$, $n = 8$, Student's *t*-test; Fig. 5*C*).

ELLA on extracted samples from human tracheal epithelial cells showed the significant amounts of SNA binding (Fig. 5*D*). Treatment with L-carbocisteine (10 μM, 72 h) reduced the levels of binding of this lectin (Fig. 5*D*).

Effects of L-carbocisteine on pH in the acidic endosomes. Acidic endosomes in human tracheal epithelial cells were stained green with LysoSensor DND-189 (Fig. 6, *A* and *B*). Treatment of the cells with L-carbocisteine (10 μM, 3 days) reduced the number of acidic endosomes with green fluorescence in the cells (Fig. 6*B*) and the fluorescence intensity from acidic endosomes in the epithelial cells (Fig. 6*C*) compared with that in cells treated with vehicle of L-carbocisteine (0.1% double-distilled water).

Effects of L-carbocisteine on cytokine production. The secretions of IL-1β, IL-6, and IL-8 all increased after FluA virus infection (Fig. 7), and maximum secretion was observed at 5 days after the infection (data at 1, 3, and 7 days not shown). Treatment with L-carbocisteine (10 μM) reduced the concentrations of IL-1β, IL-6, and IL-8 5 days after FluA virus infection as well as baseline concentrations of these cytokines before FluA virus infection (Fig. 7). In contrast, UV-irradiated influenza virus did not increase IL-1β, IL-6, and IL-8 (Fig. 7). Likewise, the secretion of IL-1β, IL-6, and IL-8 in supernatant fluids of the cells from 5 patients complicated with COPD did not differ from those from 31 patients without COPD (data not shown). The magnitude of inhibitory effects of L-carbocisteine in the cells from COPD patients was also similar to that in the cells from patients without COPD (data not shown).

Effects of L-carbocisteine on NF-κB. In the human tracheal epithelial cells before FluA virus infection, a significant amount of p50, p65, c-Rel, p52, and RelB of NF-κB was detected in the nuclear extracts. L-carbocisteine (10 μM, 3 days) significantly reduced the amount of p50, p65, c-Rel, p52, and RelB of NF-κB in the nuclear extracts in the cells (Fig. 8).

DISCUSSION

In the present study, we have shown that viral titers in supernatant fluids and RNA of FluA virus in the human tracheal epithelial cells increased with time, and L-carbocisteine reduced viral titers of FluA virus in supernatant fluids concentration-dependently, RNA of FluA virus replication in the cells, and the susceptibility to FluA virus infection. Immunocytochemical staining with FITC-labeled SNA lectin (23) and an ELLA (11, 21) showed that the cultured human tracheal epithelial cells expressed SAα2,6Gal, a receptor for human influenza virus (18). Treatment of human tracheal epithelial cells with L-carbocisteine reduced the expression of the receptor on the epithelial cells. These findings suggest that L-carbocisteine might inhibit FluA virus infection, partly through the reduced expression of the receptor for human influenza virus in the human tracheal epithelial cells. L-carbocisteine also reduced the number of acidic endosomes from which RNA of FluA enters into the cytoplasm and reduced the fluorescence intensity from acidic endosomes in the cells. These findings suggest that the reduction of acidic endosomes might also relate to the inhibition of FluA virus infection by L-carbocisteine. Furthermore, L-carbocisteine reduced concentrations of proinflammatory cytokines and a monokine, including IL-1β, IL-6, and IL-8 in supernatant fluids. L-carbocisteine may also modulate airway inflammation induced by FluA virus infection.

MDCK cells did not show any morphological change that shows the presence of FluA virus when supernatant fluids collected 1 h after FluA virus infection were added to the MDCK cells. In contrast, supernatant fluids 24 h after infection produced a morphological change on the cells showing the presence of FluA virus (15). These findings suggest that supernatant fluids 24 h after infection contained significant amounts of FluA virions, which were newly produced after infection.

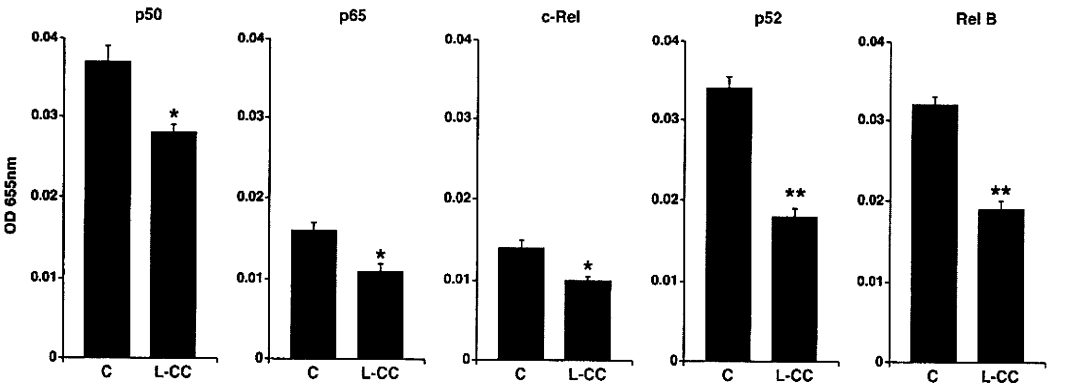

Fig. 8. Amount of p50, p65, c-Rel, p52, and RelB in nuclear extracts in human tracheal epithelial cells treated with L-carbocisteine (L-CC; 10 μM) or vehicle (C; 0.1% double-distilled water) for 3 days before FluA virus infection. Results are expressed as OD and are means ± SE from 5 different tracheae. Significant differences from control values (C) before FluA virus infection are indicated by $*P < 0.05$ and $**P < 0.01$.

Downloaded from ajplung.physiology.org on August 2, 2010

Human seasonal influenza viruses and classical H_1N_1 swine influenza viruses bind to SAα2,6Gal, and most avian and equine viruses bind to SAα2,3Gal (18). An expression of SAα2,6Gal was observed in epithelial cells in the nasal mucosa, pharynx, tracheae, and bronchi (6, 23). In contrast, SAα2,3Gal was reported not to express on the tracheal epithelial cells (6), whereas Matrosovich et al. (13) demonstrated its expression on ciliated cells in the human tracheae. SAα2,3Gal is also expressed in nonciliated cuboidal bronchiolar cells and type II cells lining the alveolar wall (23). In this study, human tracheal epithelial cells expressed SAα2,6Gal but not SAα2,3Gal (data not shown). These findings are consistent with those in previous reports (6, 13, 23). In the present study, immunocytochemistry and ELLA demonstrated the reduced expression of SAα2,6Gal in human tracheal epithelial cells after treatment with L-carbocisteine. Furthermore, the minimum dose of FluA virus necessary to cause infection in the cells treated with L-carbocisteine was significantly higher than that in the cells treated with vehicle of L-carbocisteine, showing the reduced susceptibility to FluA virus infection. These findings suggest that L-carbocisteine might reduce the amount of FluA virus virions attached on the epithelial cells through the reduced expression of SAα2,6Gal in the cells.

The mechanisms for the reduction of SAα2,6Gal expression by L-carbocisteine are uncertain. However, TNF-α, one of the inflammatory mediators in airways, increases the expression glycosyltransferase and sulfotransferase responsible for biosynthesis of sialylated epitopes in the bronchial mucosa (8) through the activation of NF-κB (4). SAα2,6Gal glycotopes on serum glycoproteins also increase in inflamed mice in response to turpentine oil (38). On the other hand, as we (37) previously demonstrated, L-carbocisteine reduces the production of proinflammatory cytokines such as IL-1 through the inhibition of NF-κB activation. We also demonstrated the inhibitory effects of L-carbocisteine on NF-κB activation in this study. These findings suggest that reduced NF-κB might be partly associated with the reduced expression of SAα2,6Gal by L-carbocisteine in the human tracheal epithelial cells.

After attachment of influenza virus to the receptor, viruses enter the airway epithelial cells and are internalized by endocytic compartments via four internalization mechanisms, including: clarthrin-coated pits; caveolae; nonclathrin, noncaveolae pathway; and macropinocytosis (17). Of these mechanisms, a nonclathrin, noncaveolae-mediated internalization pathway depends on low pH (24). Furthermore, after binding on the cell surface, the virus is internalized by receptor-mediated endocytosis, and the low pH in the endosome triggers fusion of the viral and endosomal membranes. The viruses then release their ribonucleoproteins (RNPs), including viral RNA, into the cytoplasm, resulting in the next processes of viral replication (17, 31). As shown previously (37) and in this study, L-carbocisteine reduced the number of acidic endosomes and the fluorescence intensity from acidic endosomes in the cells. Furthermore, L-carbocisteine reduced FluA viral RNA in human tracheal epithelial cells and viral titers of influenza in supernatant fluids. These findings are consistent with the reports that bafilomycin A_1 reduces the number of acidic endosomes (16, 28) in the epithelial cells and reduces the growth of influenza virus in MDCK cells (16). Increased pH in acidic endosomes might relate to the inhibition of virus entry and releasing the viral RNPs into the cytoplasm and might inhibit the next processes of viral replication in this study.

In this study, we demonstrated that L-carbocisteine reduces the expression of the receptor for FluA virus on the human tracheal epithelial cells and reduces the number of acidic endosomes from which influenza virus RNA enters into the cytoplasm. However, Yang et al. (35) demonstrated that a mucolytic agent, ambroxol, inhibits influenza virus multiplication and improves the survival rate of mice. They suggested that the inhibitory effects of ambroxol on influenza virus infection may be associated with upregulation on the production of pulmonary surfactant (2), mucus protease inhibitor (3), and immunoglobulin. Further studies are needed to examine the effects of L-carbocisteine on these mechanisms.

The inhibitory effects of L-carbocisteine on the production of proinflammatory cytokines and a monokine observed in this study are consistent with those of a previous report that L-carbocisteine reduces them in airway epithelial cells after rhinovirus infection (37). These findings are also similar to that of an in vivo study by Yang et al. (35) that ambroxol reduces these proinflammatory factors including TNF-α in mice after influenza virus infection. Influenza virus infection induces airway inflammation through the production of proinflammatory cytokines and chemokines such as IL-6, IL-8, and IP-10 (7, 30) and through epithelial cell damage, both of which are associated with exacerbations of COPD (12). Therefore, the inhibitory effects of L-carbocisteine on the production of the cytokines and chemokines may also relate to reduced frequency of exacerbations in COPD patients (36, 40).

In summary, we demonstrated that L-carbocisteine, a mucolytic agent, inhibits FluA virus infection in human tracheal epithelial cells at least by the reduced expression of the receptor on the cells and the reduction of acidic endosomes where the viral RNPs are released into the cytoplasm. L-carbocisteine may also modulate airway inflammation after influenza virus infection.

ACKNOWLEDGMENTS

We thank Grant Crittenden for reading the manuscript.

GRANTS

This study was funded by Ministry of Health, Labour, and Welfare Sciences Research Grants for Research on Measures for Intractable Diseases (H20-Nanchi-Ippan-035) from the Japanese Government and supported by Kyorin Pharmaceutical.

DISCLOSURES

M. Yamaya and H. Kubo are teachers in the Department of Advanced Preventive Medicine for Infectious Disease, Tohoku University School of Medicine. The department was funded by six pharmaceutical companies including Kyorin Pharmaceutical, and the Conflict of Interest Committee of the Tohoku University defined and confirmed that M. Yamaya and H. Kubo have no conflict of interest.

REFERENCES

1. **Beigel J, Bray M.** Current and future antiviral therapy of severe seasonal and avian influenza. *Antiviral Res* 78: 91–102, 2008.
2. **Benne CA, Kraaijeveld CA, van Strijp JA, Brouwer E, Harmsen M, Verhoef J, van Golde LM, van Iwaarden JF.** Interactions of surfactant protein A with influenza A viruses: binding and neutralization. *J Infect Dis* 171: 335–341, 1995.
3. **Beppu Y, Imamura Y, Tashiro M, Towatari T, Ariga H, Kido H.** Human mucus protease inhibitor in airway fluids is a potential defensive

Downloaded from ajplung.physiology.org on August 2, 2010

compound against infection with influenza A and Sendai viruses. *J Biochem* 121: 309–316, 1997.
4. **Chen GY, Sakuma K, Kannagi R.** Significance of NF-κB/GATA axis in tumor necrosis factor-alpha-induced expression of 6-sulfated cell recognition glycans in human T-lymphocytes. *J Biol Chem* 283: 34563–34570, 2008.
5. **Condit RC.** Principles of virology. In: *Fields Virology* (5th ed.), edited by Knipe DM and Howley PM. Philadelphia: Lippincott Williams & Wilkins, 2006, p. 25–57.
6. **Couceiro JN, Paulson JC, Baum LG.** Influenza virus strains selectively recognize sialyloligosaccharides on human respiratory epithelium: the role of the host cell in selection of hemagglutinin receptor specificity. *Virus Res* 29: 155–165, 1993.
7. **de Jong MD, Simmons CP, Thanh TT, Hien VM, Smith GJ, Chau TN, Hoang DM, Chau NV, Khanh TH, Dong VC, Qui PT, Cam BV, Ha do Q, Guan Y, Peiris JS, Chinh NT, Hien TT, Farrar J.** Fatal outcome of human influenza A (H_5N_1) is associated with high viral load and hypercytokinemia. *Nat Med* 12: 1203–1207, 2006.
8. **Delmotte P, Degroote S, Lafitte JJ, Lamblin G, Perini JM, Rousselk P.** TNF-α increases the expression of glycosyltraneferases and sulfotransferases responsible for the biosynthesis of sialylated and/or sulfated Lewis x epitopes in the human bronchial asthma. *J Biol Chem* 277: 424–431, 2002.
9. **De Schutter JA, Van der Weken G, Van den Bossche W, de Moerloose P.** Determination of *S*-carbomethylcysteine in serum by reversed-phase ion-pair liquid chromatography with column switching following precolumn derivatization with *o*-phtalaldehyde. *J Chromatogr A* 428: 301–310, 1988.
10. **Fiorucci S, Antonelli E, Distrutti E, Del Soldato P, Flower RJ, Clark MJ, Morelli A, Perretti M, Ignarro LJ.** NCX-1015, a nitric-oxide derivative of prednisolone, enhances regulatory T cells in the lamina propria and protects against 2,4,6-trinitrobenzene sulfonic acid-induced colitis in mice. *Proc Natl Acad Sci USA* 99: 15770–15775, 2002.
11. **Gagneux P, Cheriyan M, Hurtado-Ziola N, van der Linden EC, Anderson D, McClure H, Varki A, Varki NM.** Human-specific regulation of alpha 2–6-linked sialic acids. *J Biol Chem* 278: 48245–48250, 2003.
12. **Johnston SL.** Overview of virus-induced airway disease. *Proc Am Thorac Soc* 2: 150–156, 2005.
13. **Matrosovich MN, Matrosovich TY, Gray T, Roberts NA, Klenk HD.** Human and avian influenza viruses target different cell types in cultures of human airway epithelium. *Proc Natl Acad Sci USA* 101: 4620–4624, 2004.
14. **Nichol KL, Margolis KL, Wuorenma J, Von Sternberg T.** The efficacy and cost effectiveness of vaccination against influenza among elderly persons living in the community. *N Engl J Med* 331: 778–784, 1994.
15. **Numazaki Y, Oshima T, Ohmi A, Tanaka A, Oizumi Y, Komatsu S, Takagi T, Karahashi M, Ishida N.** A microplate method for isolation of viruses from infants and children with acute respiratory infections. *Microbiol Immunol* 31: 1085–1095, 1987.
16. **Ochiai H, Sakai S, Hirabayashi T, Shimizu Y, Terasawa K.** Inhibitory effect of bafilomycin A_1, a specific inhibitor of vacuolar-type proton pump, on the growth of influenza A and B viruses in MDCK cells. *Antiviral Res* 27: 425–430, 1995.
17. **Palese P, Shaw ML.** Orthomyxoviridae. In: *Fields Virology* (5th ed.), edited by Knipe DM and Howley PM. Philadelphia: Lippincott Williams & Wilkins, 2006, p. 1647–1689.
18. **Rogers GN, Paulson JC.** Receptor determinants of human and animal influenza virus isolates: differences in receptor specificity of the H_3 hemagglutinin based on species of origin. *Virology* 127: 361–373, 1983.
19. **Rohde G, Wiethege A, Borg I, Kauth M, Bauer TT, Gillissen A, Bufe A, Schultze-Werninghaus G.** Respiratory viruses in exacerbations of chronic obstructive pulmonary disease requiring hospitalisation: a case-control study. *Thorax* 58: 37–42, 2003.
20. **Sakakura Y, Majima Y, Saida S, Ukai K, Miyoshi Y.** Reversibility of reduced mucociliary clearance in chronic sinusitis. *Clin Otolaryngol Allied Sci* 10: 79–83, 1985.
21. **Sandberg T, Mellin L, Gelius U, Caldwell KD.** Surface analysis of pure and complex mucin coatings on a real-type substrate using individual and combined mBCA, ELLA, and ELISA. *J Colloid Interface Sci* 333: 180–187, 2009.
22. **Sethi S.** New developments in the pathogenesis of acute exacerbations of chronic obstructive pulmonary disease. *Curr Opin Infect Dis* 17: 113–119, 2004.
23. **Shinya K, Ebina M, Yamada S, Ono M, Kasai N, Kawaoka Y.** Influenza virus receptors in the human airway. *Nature* 440: 435–436, 2006.
24. **Sieczkarski SB, Whittaker GR.** The role of protein kinase C βII in influenza virus entry via late endosomes. *J Virol* 77: 460–469, 2003.
25. **Spackman E, Senne DA, Myers TJ, Bulaga LL, Garber LP, Perdue ML, Lohman K, Daum LT, Suarez DL.** Development of a real-time reverse transcriptase PCR assay for type A influenza virus and the avian H_5 and H_7 hemagglutinin subtypes. *J Clin Microbiol* 40: 3256–3260, 2002.
26. **Subauste MC, Jacoby DB, Richards SM, Proud D.** Infection of a human respiratory epithelial cell line with rhinovirus. Induction of cytokine release and modulation of susceptibility to infection by cytokine exposure. *J Clin Invest* 96: 549–557, 1995.
27. **Sueyoshi S, Miyata Y, Masumoto Y, Ishibashi Y, Matsuzawa S, Harano N, Tsuru K, Imai S.** Reduced airway inflammation and remodeling in parallel with mucin 5AC protein expression decreased by *S*-carboxymethylcysteine, a mucoregulant, in the airways of rats exposed to sulfur dioxide. *Int Arch Allergy Immunol* 134: 273–280, 2004.
28. **Suzuki T, Yamaya M, Sekizawa K, Hosoda M, Yamada N, Ishizuka S, Nakayama K, Yanai M, Numazaki Y, Sasaki H.** Bafilomycin A_1 inhibits rhinovirus infection in human airway epithelium: effects on endosome and ICAM-1. *Am J Physiol Lung Cell Mol Physiol* 280: L1115–L1127, 2001.
29. **Suzuki T, Yamaya M, Sekizawa K, Hosoda K, Yamada N, Ishizuka S, Yoshino A, Yasuda H, Takahashi H, Nishimura H, Sasaki H.** Erythromycin inhibits rhinovirus infection in cultured human tracheal epithelial cells. *Am J Respir Crit Care Med* 165: 1113–1118, 2002.
30. **Van Lenten BJ, Wagner AC, Navab M, Anantharamaiah GM, Hui EK, Nayak DP, Fogelman AM.** D-4F, an apolipoprotein A-I mimetic peptide, inhibits the inflammatory response induced by influenza A infection of human type II pneumocytes. *Circulation* 110: 3252–3258, 2004.
31. **White J, Kielian M, Helenius A.** Membrane fusion proteins of enveloped animal viruses. *Q Rev Biophys* 16: 151–195, 1983.
32. **Widdicombe JH, Coleman DL, Finkbeiner WE, Friend DS.** Primary cultures of the dog's tracheal epithelium: fine structure, fluid, and electrolyte transport. *Cell Tissue Res* 247: 95–103, 1987.
33. **Yamaya M, Finkbeiner WE, Chun SY, Widdicombe JH.** Differentiated structure and function of cultures from human tracheal epithelium. *Am J Physiol Lung Cell Mol Physiol* 262: L713–L724, 1992.
34. **Yamaya M, Sasaki T, Yasuda H, Inoue D, Suzuki T, Asada M, Yoshida M, Seki T, Iwasaki K, Nishimura H, Nakayama K.** Hochu-ekki-to inhibits rhinovirus infection in human tracheal epithelial cells. *Br J Pharmacol* 150: 702–710, 2007.
35. **Yang B, Yao DF, Ohuchi M, Ide M, Yano M, Okumura Y, Kido H.** Ambroxol suppresses influenza-virus proliferation in the mouse airway by increasing antiviral factor levels. *Eur Respir J* 19: 952–958, 2002.
36. **Yasuda H, Yamaya M, Sasaki T, Inoue D, Nakayama K, Tomita N, Yoshida M, Sasaki H.** Carbocisteine reduces frequency of common colds and exacerbations in COPD patients. *J Am Geriatr Soc* 54: 378–380, 2006.
37. **Yasuda H, Yamaya M, Sasaki T, Inoue D, Nakayama K, Yamada M, Suzuki T, Sasaki H.** Carbocisteine inhibits rhinovirus infection in human tracheal epithelial cells. *Eur Respir J* 28: 51–58, 2006.
38. **Yasukawa Z, Sato C, Kitajima K.** Inflammation-dependent changes in α2,3-, α2,6-, and α2,8-sialic acid glycotopes on serum glycoproteins in mice. *Glycobiology* 15: 827–837, 2005.
39. **Zafarullah M, Li WQ, Sylvester J, Ahmad M.** Molecular mechanisms of *N*-acetylcysteine actions. *Cell Mol Life Sci* 60: 6–20, 2003.
40. **Zheng JP, Kang J, Huang SG, Chen P, Yao WZ, Yang L, Bai CX, Wang CZ, Wang C, Chen BY, Shi Y, Liu CT, Chen P, Li Q, Wang ZS, Huang YJ, Luo ZY, Chen FP, Yuan JZ, Yuan BT, Qian HP, Zhi RC, Zhong NS.** Effect of carbocisteine on acute exacerbation of chronic obstructive pulmonary disease (PEACE Study): a randomised placebo-controlled study. *Lancet* 371: 2013–2018, 2008.

Downloaded from ajplung.physiology.org on August 2, 2010

Jpn. J. Infect. Dis., 62, 392-393, 2009

Short Communication

The Effects of an Hsp90 Inhibitor on the Paradoxical Effect

Yukihiro Kaneko*, Hideaki Ohno, Yoshifumi Imamura[1], Shigeru Kohno[1], and Yoshitsugu Miyazaki

Department of Chemotherapy and Mycoses, National Institute of Infectious Diseases, Tokyo 162-8640; and [1]Department of Molecular Microbiology and Immunology, Nagasaki University Graduate School of Biomedical Sciences, Nagasaki 852-8501, Japan

(Received April 28, 2009. Accepted August 18, 2009)

SUMMARY: It is important to conserve the effectiveness of antifungal agents because the options for currently available agents are limited. Although echinocandins, which have been developed in recent decades, are highly active against a broad spectrum of fungi, one concern is their reduced activity against *Candida albicans* at high drug concentrations, which is known as the paradoxical effect. To date, resistance related to the paradoxical effect has not been reported in clinical situations, but some in vivo data suggest that the paradoxical effect potentiates the emergence of resistance. It is valuable to investigate the underlying mechanisms of as well as strategies against this paradoxical resistance. Previous reports imply that the paradoxical effect might be related to stress responses. In this study, we report that radicicol, a heat shock protein 90 (Hsp90) inhibitor, reduces the paradoxical effect of micafungin. We also confirm that radicicol reduces the tolerance to voriconazole, one of the new azoles, which is consistent with a previous report. Our results may therefore imply that common stress responses might exist in the paradoxical resistance to micafungin and also the tolerance to voriconazole, and may suggest that inhibiting Hsp90-related stress responses could help to avoid potential resistances.

The emergence of resistance is one of the problems in intractable infections such as fungal infections. Because the options for currently available antifungal agents are still limited, it is important to maintain the effectiveness of these agents against fungi as long as possible (1,2). Though echinocandins have been developed in recent decades and are highly active against a broad spectrum of fungi, including *Candida* and *Aspergillus* spp., there are concerns regarding their reduced activity at high drug concentrations, which is known as the paradoxical effect (PE) (3). To date, the PE has been linked to upregulation of homeostatic cell wall stress responses such as calcineurin (4,5). Since heat shock protein 90 (Hsp90) is one of the key stress response components, we investigated whether an inhibitor of Hsp90 could reduce the PE of *Candida albicans*.

SC5314, a standard *C. albicans* strains from our collection, was used in this study (6). Micafungin (MFG), one of the echinocandins, and voriconazole (VRC), one of the new azoles, were kindly provided from Astellas Pharma Inc. (Tokyo, Japan) and Pfizer Japan Inc. (Tokyo, Japan), respectively. Radicicol (Rad, Hsp90 inhibitor; MIC = 8 μM) was purchased from Sigma-Aldrich (St. Louis, Mo., USA). MFG was dissolved in distilled water, and VRC and Rad were dissolved in dimethylsulfoxide (DMSO) for stock solutions, and they were stored at −20°C before use. We used yeast nitrogen base medium (YNB) (Difco Laboratories, Detroit, Mich., USA) instead of RPMI medium, which is recommended as a standard medium by the Clinical and Laboratory Standards Institute (CLSI) because growth is slow in RPMI, making it difficult to detect paradoxical growth.

After overnight preculture in YNB supplemented with 2% glucose, approximately 2×10^3 cells were inoculated in each well of 96-well plates. Each well contained 200 μl of YNB with the indicated concentrations of MFG or VRC; without Rad or with 1 μM Rad. The maximum final DMSO concentration (0.1%) was included in assays performed in the absence of Rad to control for any solvent effects. After a 24-h incubation period, the cell growth was compared using an XTT assay. Though the XTT assay is not usually used for examining planktonic cell growth, this assay is useful for detecting small amounts of cell growth such as that occurring with paradoxical growth because it is more sensitive than simple optical density measurements. The method was slightly modified from that previously described (7). In brief, the plates were centrifuged to spin down the organisms, the medium was removed, and 200 μl of PBS containing 50 μg/ml of XTT (Sigma-Aldrich) and 4 μM menadione (Sigma-Aldrich) was added to each well. After a 1-h incubation period, the absorbance at 490 nm/630 nm was measured by plate reader and values were normalized to the control (neither an antifungal agent nor Rad) as the relative cell growth. Each condition was quadruplicated. *P* values were calculated using the Student's unpaired *t* test.

As previously described for the PE, MFG severely inhibited cell growth to less than 1% at 0.031 and 0.063 μg/ml, and higher concentrations of MFG were less effective (Fig. 1A). The addition of 1 μM Rad, which alone did not alter growth, reduced the paradoxical cell growth at high concentrations of MFG. We confirmed that cyclosporin A, which is a calcineurin inhibitor, also attenuated the PE, as previously described (4) (data not shown). These results are consistent with the results from previous studies showing the relationship between the PE and stress-related cell integrity pathways (3-5,8,9). Rad also reduced the tolerance to VRC, as previously noted (Fig. 1B) (10). These results may suggest that the paradoxical resistance to MFG depends on the same stress responses as the tolerance to VRC.

Cowen et al. first reported that an Hsp90 inhibitor did not alter the sensitivity to caspofungin, an echinocandin, but they also recently reported that an Hsp90 inhibitor enhanced the

*Corresponding author: Mailing address: Department of Chemotherapy and Mycoses, National Institute of Infectious Diseases, Toyama 1-23-1, Shinjuku-ku, Tokyo 162-8640, Japan. Tel: +81-3-5285-1111 (2327), Fax: +81-3-5285-1272, E-mail: ykaneko@nih.go.jp

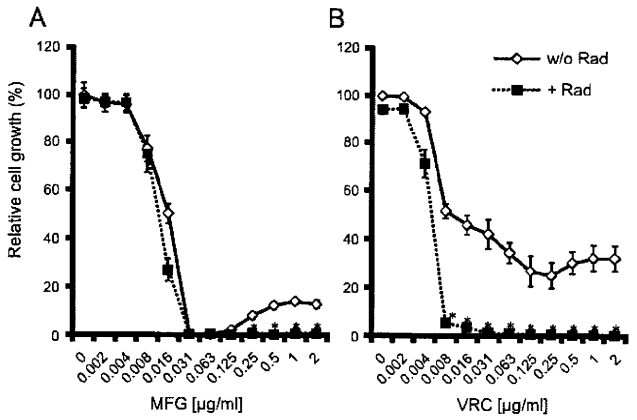

Fig. 1. Relative cell growth at various concentrations of MFG (A) or VRC (B); when used without Rad (w/o Rad) or with 1 μM Rad (+ Rad). All values are as a percentage of cell growth (XTT activity) in a control with neither antifungal agent nor Rad.
*$P < 0.01$ compared to corresponding value without Rad.
MFG, micafungin; VRC, voriconazole; Rad, radicicol.

fungicidal effects of MFG (10,11). Their latter finding might be related to our results.

It remains controversial whether the PE phenotype is clinically important. Only a mutation of *fks1*, which is a target of echinocandins, has been proven to cause clinical failure with echinocandins to date, and it has been reported that the PE is not due to the *fks1* mutation (9,12,13). However, some studies have found the PE in vivo as well as in vitro, and accordingly it is not deniable that the PE potentiates the threat of clinically relevant resistance (14-17). Therefore, inhibiting the PE may be important for avoiding the emergence of resistance, and regulating stress responses could be useful for inhibiting the PE.

In conclusion, the present findings regarding the PE and the development of resistance in antifungal agents could be valuable. It has never before been reported that an Hsp90 inhibitor reduces the PE, and this finding may suggest that inhibiting Hsp90-related stress responses could help to avoid potential resistances.

ACKNOWLEDGMENTS

This work was partly supported by the Ministry of Education, Culture, Sports, Science and Technology of Japan (KAKENHI 20591212 and KAKENHI 20790714), the Ministry of Health, Labour and Welfare of Japan (H20shinkouippan012, H20nanchiippan035 and H20shinkouippan015) and Japan Health Science Foundation (KHC3333).

REFERENCES

1. Ruhnke, M., Hartwig, K. and Kofla, G. (2008): New options for treatment of candidaemia in critically ill patients. Clin. Microbiol. Infect., 14 (Suppl. 4), 46-54.
2. Carrillo-Munoz, A.J., Giusiano, G., Ezkurra, P.A., et al. (2006): Antifungal agents: mode of action in yeast cells. Rev. Esp. Quimioter., 19, 130-139.
3. Wiederhold, N.P. (2007): Attenuation of echinocandin activity at elevated concentrations: a review of the paradoxical effect. Curr. Opin. Infect. Dis., 20, 574-578.
4. Wiederhold, N.P., Kontoyiannis, D.P., Prince, R.A., et al. (2005): Attenuation of the activity of caspofungin at high concentrations against *Candida albicans*: possible role of cell wall integrity and calcineurin pathways. Antimicrob. Agents Chemother., 49, 5146-5148.
5. Walker, L.A., Munro, C.A., de Bruijn, I., et al. (2008): Stimulation of chitin synthesis rescues *Candida albicans* from echinocandins. PLoS Pathog., 4, e1000040.
6. Jones, T., Federspiel, N.A., Chibana, H., et al. (2004): The diploid genome sequence of *Candida albicans*. Proc. Natl. Acad. Sci. USA, 101, 7329-7334.
7. Melo, A.S., Colombo, A.L. and Arthington-Skaggs, B.A. (2007): Paradoxical growth effect of caspofungin observed on biofilms and planktonic cells of five different *Candida* species. Antimicrob. Agents Chemother., 51, 3081-3088.
8. Truman, A.W., Millson, S.H., Nuttall, J.M., et al. (2007): In the yeast heat shock response, Hsf1-directed induction of Hsp90 facilitates the activation of the Slt2 (Mpk1) mitogen-activated protein kinase required for cell integrity. Eukaryot. Cell, 6, 744-752.
9. Stevens, D.A., Ichinomiya, M., Koshi, Y., et al. (2006): Escape of *Candida* from caspofungin inhibition at concentrations above the MIC (paradoxical effect) accomplished by increased cell wall chitin; evidence for beta-1,6-glucan synthesis inhibition by caspofungin. Antimicrob. Agents Chemother., 50, 3160-3161.
10. Cowen, L.E. and Lindquist, S. (2005): Hsp90 potentiates the rapid evolution of new traits: drug resistance in diverse fungi. Science, 309, 2185-2189.
11. Singh, S.D., Robbins, N., Zaas, A.K., et al. (2009): Hsp90 governs echinocandin resistance in the pathogenic yeast *Candida albicans* via calcineurin. PLoS Pathog., 5, e1000532.
12. Kanafani, Z.A. and Perfect, J.R. (2008): Antimicrobial resistance: resistance to antifungal agents: mechanisms and clinical impact. Clin. Infect. Dis., 46, 120-128.
13. Chamilos, G., Lewis, R.E., Albert, N., et al. (2007): Paradoxical effect of echinocandins across *Candida* species in vitro: evidence for echinocandin-specific and *Candida* species-related differences. Antimicrob. Agents Chemother., 51, 2257-2259.
14. Lewis, R.E., Albert, N.D. and Kontoyiannis, D.P. (2008): Comparison of the dose-dependent activity and paradoxical effect of caspofungin and micafungin in a neutropenic murine model of invasive pulmonary aspergillosis. J. Antimicrob. Chemother., 61, 1140-1144.
15. Clemons, K.V., Espiritu, M., Parmar, R., et al. (2006): Assessment of the paradoxical effect of caspofungin in therapy of candidiasis. Antimicrob. Agents Chemother., 50, 1293-1297.
16. Wiederhold, N.P., Kontoyiannis, D.P., Chi, J., et al. (2004): Pharmacodynamics of caspofungin in a murine model of invasive pulmonary aspergillosis: evidence of concentration-dependent activity. J. Infect. Dis., 190, 1464-1471.
17. Stevens, D.A., Espiritu, M. and Parmar, R. (2004): Paradoxical effect of caspofungin: reduced activity against *Candida albicans* at high drug concentrations. Antimicrob. Agents Chemother., 48, 3407-3411.

Journal of Medical Virology 81:1951–1958 (2009)

Detection of Merkel Cell Polyomavirus in Merkel Cell Carcinoma and Kaposi's Sarcoma

Harutaka Katano,[1]* Hideki Ito,[2] Yoshio Suzuki,[3] Tomoyuki Nakamura,[1] Yuko Sato,[1] Takahiro Tsuji,[1] Koma Matsuo,[2] Hidemi Nakagawa,[2] and Tetsutaro Sata[1]

[1]Department of Pathology, National Institute of Infectious Diseases, Shinjuku, Tokyo, Japan
[2]Department of Dermatology, Jikei University School of Medicine, Minato, Tokyo, Japan
[3]Department of Pathology, Asahi General Hospital, Asahi, Chiba, Japan

Merkel cell carcinoma is a rare malignancy that sometimes occurs in the skin of elderly people. Recently, a new human polyomavirus, Merkel cell polyomavirus (MCPyV) was identified in Merkel cell carcinoma. In the present study, MCPyV-DNA was detected in 6 of 11 (55%) cases of Merkel cell carcinoma by nested PCR and real-time PCR. Histologically, MCPyV-positive cases showed round and vesicular nuclei with a fine granular chromatin and small nucleoli, whereas MCPyV-negative cases showed polygonal nuclei with diffusely distributed chromatin. Real-time PCR analysis to detect the MCPyV gene revealed that viral copy numbers ranged 0.04–0.43 per cell in cases of Merkel cell carcinoma. MCPyV was also detected in 3 of 49 (6.1%) cases of Kaposi's sarcoma (KS), but not in 192 DNA samples of other diseases including 142 autopsy samples from 20 immunodeficient patients. The MCPyV copy number in KS was lower than that in Merkel cell carcinoma. PCR successfully amplified a full-length MCPyV genome from a case of KS. Sequence analysis revealed that the MCPyV isolated from KS had 98% homology to the previously reported MCPyV genomes. These data suggest that the prevalence of MCPyV is low in Japan, and is at least partly associated with the pathogenesis of Merkel cell carcinoma. ***J. Med. Virol. 81:1951–1958, 2009.***

© 2009 Wiley-Liss, Inc.

KEY WORDS: Merkel cell polyomavirus; Merkel cell carcinoma; real-time PCR; Kaposi's sarcoma

INTRODUCTION

Merkel cell carcinoma is a rare skin malignancy that originates in the Merkel cell, a neuroendocrine cell in the skin [Skelton et al., 1997; Pectasides et al., 2006; Lemos and Nghiem, 2007]. Merkel cell carcinoma is an aggressive skin cancer that commonly occurs on sun-exposed areas of elderly people. The incidence of Merkel cell carcinoma is high in Caucasians, but lower in other races [Agelli and Clegg, 2003]. Typical histology of Merkel cell carcinoma shows that the tumor consists of small, round cells with vesicular nuclei, fine chromatin, and minimal cytoplasm. Because these morphological features are similar to other small cell tumors such as small cell lung cancer and lymphoma, immunohistochemistry for cytokeratin 20 is often useful for differential diagnosis. Recurrence and metastasis in the regional lymph nodes are observed in up to 30% of cases [Agelli and Clegg, 2003]. Merkel cell carcinoma comprises two subtypes, "classic" and "variant," based on clinical manifestations and gene expression profiles [Van Gele et al., 2004; Fernandez-Figueras et al., 2007]. Gene expression profiling studies have also demonstrated that metastasis of Merkel cell carcinoma is correlated with the over-expression of some metastasis-associated proteins such as matrix metalloproteinases [Fernandez-Figueras et al., 2007].

A new human polyomavirus, Merkel cell polyomavirus (MCPyV), was identified recently in samples of Merkel cell carcinoma by digital transcriptome subtraction [Feng et al., 2008]. MCPyV is a 5.4-kbp long, double-stranded DNA virus and has high

Grant sponsor: Health and Labor Sciences Research Grants from the Ministry of Health, Labor and Welfare; Grant numbers: H21-AIDS-Ippan-006 (partial support to H.K.), H19-AIDS-Ippan-003 (to H.K.); H20-Nanchi-Ippan-035 (to T.S.); H20-Shinko-Ippan-006 (to T.S.); Grant sponsor: Ministry of Education, Culture, Sports, Science and Technology of Japan (to H.K.); Grant number: 21590520; Grant sponsor: Research on Health Sciences Focusing on Drug Innovation from the Japan Health Sciences Foundation (to H.K. and T.S.); Grant number: SAA4832.

*Correspondence to: Harutaka Katano, Department of Pathology, National Institute of Infectious Diseases, 1-23-1 Toyama, Shinjuku, Tokyo 162-8640, Japan. E-mail: katano@nih.go.jp

Accepted 29 June 2009
DOI 10.1002/jmv.21608
Published online in Wiley InterScience (www.interscience.wiley.com)

© 2009 WILEY-LISS, INC.

homology to murine, African green monkey, and hamster polyomaviruses. The MCPyV genome encodes a large T antigen, which contains some conserved domains that were shown previously to play roles in cell transformation. In an earlier report, MCPyV was detected in 8 out of 10 cases of Merkel cell carcinoma (80%) by PCR, and clonal integration into the human genome was observed in 6 of the 8 cases with Merkel cell carcinoma [Feng et al., 2008]. Several recent reports have demonstrated the presence of MCPyV in Merkel cell carcinoma cases in the United States, Europe, and Australia, but is rare in other samples such as melanoma, skin cancer, other cancers, and controls [Foulongne et al., 2008; Giraud et al., 2008; Kassem et al., 2008; Becker et al., 2009; Bialasiewicz et al., 2009; Bluemn et al., 2009; Duncavage et al., 2009; Garneski et al., 2009; Goh et al., 2009; Ridd et al., 2009; Sharp et al., 2009]. A study using frozen samples of Merkel cell carcinoma demonstrated that all Merkel cell carcinoma samples were positive for MCPyV-DNA [Sastre-Garau et al., 2009]. These data strongly suggest that MCPyV infection is associated with the pathogenesis of Merkel cell carcinoma [zur Hausen, 2008]. On the other hand, studies using paraffin-embedded tissues suggest the presence of some MCPyV-negative cases of Merkel cell carcinoma [Foulongne et al., 2008; Kassem et al., 2008; Becker et al., 2009; Duncavage et al., 2009; Garneski et al., 2009]. In addition, MCPyV is less frequently present in Merkel cell carcinoma in Australian cases than in North American cases, suggesting geographic differences of MCPyV distribution [Garneski et al., 2009]. Although there are no accurate statistical data, Merkel cell carcinoma seems to be rare in Japan. In this study, the presence of MCPyV was investigated in Japanese cases of Merkel cell carcinoma and other diseases.

MATERIALS AND METHODS

Specimens

Studies using human tissue were performed with the approval of the Institutional Review Board of the National Institute of Infectious Diseases (Approval No. 149). Thirteen formalin-fixed paraffin-embedded tissue samples of Merkel cell carcinoma were collected from 11 patients (Table I). All of the samples were taken by biopsy or from tumor resection, and were enriched in tumor cells. The diagnosis of Merkel cell carcinoma was based on morphology and immunohistochemistry of cytokeratin 20. In addition to the Merkel cell carcinoma samples, 49 DNA samples of Kaposi's sarcoma (KS) and 50 DNA samples from tissues with various diseases were collected. A further 142 DNA samples were extracted from various organs of 20 autopsy cases with AIDS. All these human samples were archived as anonymous specimens held at the Department of Pathology, National Institute of Infectious Diseases. DNA extracted from 15 cell lines was also investigated.

TABLE I. MCPyV Infection in Merkel Cell Carcinoma Cases

Clinical information				Nested PCR for MCPyV						Real-time PCR		
Case	Sex	Age	Site	ST	LT (1017–1170)	LT (2057–2107)	VP1	VP2	VP3	MCPyV copy per 100 ng DNA	β-Actin copy per 100 ng DNA	Predicted MCPyV copy per cell
1	F	89	Cheek	−	−	−	−	−	−	0	17,505	0.000
2	F	104	Cheek	+	+	+	+	+	+	356	1,645	0.433
3	F	76	Forearm	+	+	−	−	−	+	247	12,980	0.038
4	F	50	Face	+	+	+	+	+	+	617	7,300	0.169
5	M	87	Face	−	−	−	−	−	−	0	2,053	0.000
6	M	90	Head	−	−	−	−	−	−	0	670	0.000
7	F	89	Face	−	−	−	−	−	−	0	11,940	0.000
8	F	95	Inguinal	−	−	−	−	−	−	0	39,865	0.000
8*	F	95	Abdomen	−	−	−	−	−	−	0	13,520	0.000
9	F	86	Face	+	+	+	+	+	+	691	18,960	0.073
9*	F	86	Face	+	+	−	+	+	+	78	2,796	0.056
10	M	78	Forearm	+	+	−	+	+	+	93	911	0.206
11	F	96	Cheek	+	+	−	+	−	−	50	423	0.119

Samples 8* and 9* are recurrent tumors of cases 8 and 9, respectively.